

Carbene Complexes

Gold(I) Complexes Stabilized by Nine- and Ten-Membered N-Heterocyclic Carbene Ligands

Alejandro Cervantes-Reyes,^[a] Frank Rominger⁺,^[a] Matthias Rudolph,^[a] and A. Stephen K. Hashmi^{*[a, b]}

Abstract: Nine- and ten-membered N-heterocyclic carbene (NHC) ligands have been developed and for the first time their gold(I) complexes were synthesized. The protonated NHC pro-ligands **2a–h** were prepared by the reaction of readily available *N,N'*-diarylformamidines with bis-electrophilic building blocks, followed by anion exchange. In situ deprotonation of the tetrafluoroborates **2a–h** with *t*BuOK in

the presence of AuCl(SMe₂) provided fast access to NHC-gold(I) complexes **3–10**. These new NHC-gold(I) complexes show very good catalytic activity in a cycloisomerization reaction (0.1 mol% catalyst loading, up to 100% conversion) and their solid-state structures reveal high steric hindrance around the metal atom (%*V*_{bur} up to 53.0) which is caused by their expanded-ring architecture.

Introduction

The chemistry of N-heterocyclic carbenes (NHC) has become a major area of research, because these stable carbenes have proven to be outstanding ligands for transition metals.^[1] These ligands also offer certain advantages, such as their thermal stability, low toxicity, and stability against oxidation, enabling their application in many different classes of metal-mediated reactions.^[2] Among them, NHC-gold(I) complexes^[3] have shown good catalytic activities^[4] in the activation of alkynes or alkenes for nucleophilic additions, leading to cyclizations, cycloadditions, or heteroatom additions.^[5,6] Overall, homogeneous gold catalysis has become an important tool in all fields of synthetic organic chemistry as one of the fast-growing sectors of modern chemistry.^[7] Accordingly, the development of NHC ligands for gold(I)^[7h] is an important goal, given the strong σ -donating capability of these species, to which the different re-

activity and selectivity of the gold(I) complexes can be ascribed.^[8,9]

In the last few years, the synthesis and application of a new type of NHC ligands, containing a backbone ring with more than five atoms, has emerged.^[10] These expanded-ring NHC ligands demonstrated unique steric and electronic properties in comparison with the traditional five-membered counterparts.^[11] Complexes of this class, with a broad variety of metal atoms (e.g. Cu, Ni, Fe, Pd, Pt, Ir, Rh, Ga, In) can be found in the current literature.^[11b,12] Nevertheless, only a few expanded-ring NHC-gold(I) complexes have been presented up to now (Figure 1).^[9,11a,13,14] To the best of our knowledge, no NHC-gold(I) complexes with a ring size larger than eight have been reported to date, thus their chemistry represents an intriguing field to be explored.

In this contribution we report the synthesis of the first nine- and ten-membered ring NHC ligands featuring biphenyl and diphenyl ether moieties at the backbone, and the preparation of their gold(I) complexes. The structural characteristics of both NHC salts and metal complexes are investigated, and a preliminary survey of the catalytic activity of gold(I) complexes **3–10** on the cycloisomerization of a N-propargyl carboxamide is presented.

Results and Discussion

Expanded-ring NHC pro-ligands

Various reaction conditions have been previously reported for the synthesis of six- and seven-membered protonated NHC salts, including the classic ring-closure of a disubstituted alkyl or aryl amino moiety with a pre-carbenic unit (e.g. HC(OEt)₃ or formaldehyde).^[15] Despite the good yields, those conditions are limited with regard to the bulkiness of the N-substituted backbone. Larger eight-membered ring NHC salts have been syn-

[a] A. Cervantes-Reyes, Dr. F. Rominger,⁺ Dr. M. Rudolph, Prof. Dr. A. S. K. Hashmi
Organisch-Chemisches Institut, Heidelberg University
Im Neuenheimer Feld 270, 69120 Heidelberg
(Germany)
E-mail: hashmi@hashmi.de
Homepage: <http://www.hashmi.de>

[b] Prof. Dr. A. S. K. Hashmi
Chemistry Department, Faculty of Science
King Abdulaziz University
Jeddah 21589 (Saudi Arabia)

[†] Crystallographic investigation.

Supporting Information and the ORCID identification number(s) for the author(s) of this article can be found under:
<https://doi.org/10.1002/chem.201902458>.

© 2019 The Authors. Published by Wiley-VCH Verlag GmbH & Co. KGaA. This is an open access article under the terms of the Creative Commons Attribution-NonCommercial-NoDerivs License, which permits use and distribution in any medium, provided the original work is properly cited, the use is non-commercial and no modifications or adaptations are made.

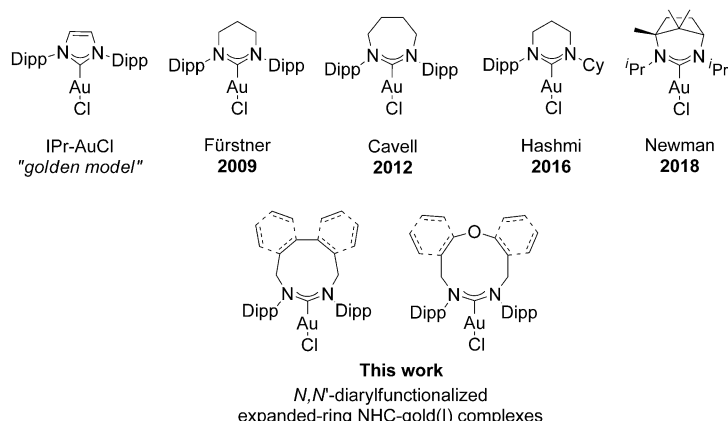
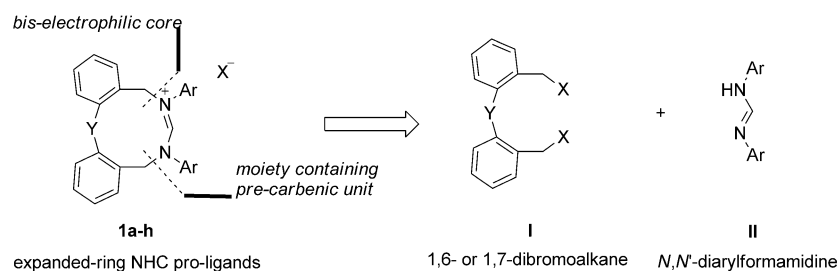


Figure 1. Milestones in the development of NHC-gold(I) complexes with NHC rings containing more than five atoms.

thesized by the reaction of a functionalized formamidine with a dihaloalkane moiety, typically in the presence of a base in a polar solvent.^[1c,4,10] In pursuit of these reported protocols, we envisioned that the new NHC pro-ligands with expanded backbone might be generated through formamidine ring-closure. Therefore, this approach was employed to synthesize the ami-

dinium salts **1a–h** starting from dibromoalkane **I** and a series of *N,N'*-diarylformamidines **II** (Scheme 1).

Our initial experiments followed well-known literature methods; for instance, employing reaction conditions reported by Jazzar et al. (*n*BuLi/hexane, THF, r.t.)^[1b] and Kolychev et al. (DIPEA, DMF, 120 °C),^[16] the expected nine- and ten-membered cyclic amidinium bromides were not obtained. By heating a mixture of dibromide **I** and *N,N'*-dimesitylformamidine at reflux, in presence of K₂CO₃ in CH₃CN for 24 h, as reported by Iglesias et al.,^[1c] we obtained the desired amidinium bromides, but in low yields (< 12 %). Recently Huynh and co-workers^[12e] synthesized various eight-membered NHC salts by isolating the monoalkylated synthetic intermediates (compound **A** in Table 1) and conducting the cyclization of the medium-sized eight-membered ring in a second step however, despite the addition of NaI to accelerate the reaction, yields were not significantly improved. Guided by those observations, we decided to increase the reaction time and work in diluted solutions (0.005 mol L⁻¹) for the challenging synthesis of the nine- and ten-membered rings; first at room temperature and



Scheme 1. Synthetic strategy for the synthesis of NHC pro-ligands **1a–h**.

Table 1. Synthesis of amidinium bromides 1a–h .				
Ar	Y	Product		Yield [%] ^[a]
2,4,6-trimethylphenyl (Mes)	none	[(9-Mes)H][Br]	1a	69
2,6-diisopropylphenyl (Dipp)	O	[(10-Mes)H][Br]	1e	48
2,6-dimethylphenyl (Xyl)	none	[(9-Dipp)H][Br]	1b	54
2,6-diethylphenyl (Dietph)	O	[(10-Dipp)H][Br]	1f	45
	none	[(9-Xyl)H][Br]	1c	84
	O	[(10-Xyl)H][Br]	1g	48
	none	[(9-Dietph)H][Br]	1d	66
	O	[(10-Dietph)H][Br]	1h	51

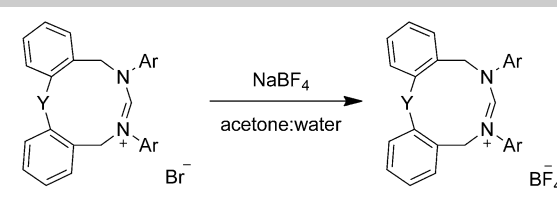
[a] Reaction conditions: Dibromoalkane **I** (1.1 mmol), *N,N'*-diarylformamidine **II** (1.0 mmol, 1.0 equiv), K₂CO₃ (1.0 equiv), CH₃CN (400 mL), r.t., 24 h, then 85 °C, 3–4 days.

then under conventional heating, to induce a full consumption of the dibromide. The yields increased considerably with this optimized procedure (45–84%, Table 1).

In general, the yields of the nine-membered NHC salts (**1a–d**, 54–84%) are notably higher than those of the ten-membered ones (**1e–h**, 45–51%). The less sterically hindered representative (**1e**, 84%) is obtained in a higher yield than the sterically more hindered one (**1b**, 54%). The resulting bromides **1a–h** are air-stable colorless to slightly colored solids that can be easily purified by recrystallization and stored at ambient conditions for weeks.

Anion exchange at **1a–h** with NaBF₄ in an acetone/water mixture smoothly produced the tetrafluoroborates **2a–h** in excellent yields (Table 2). The tetrafluoroborate anion has a lower ability to coordinate to the amidinium proton than bromide,^[1c] presumably because the bromide anion is bonded to the amidinium proton through a hydrogen bond,^[12d] and thus, the subsequent deprotonation reaction occurs more efficiently. The resulting tetrafluoroborate salts are usually colorless solids and no further recrystallization is needed. In some cases, crystalline salts can be observed due to presence of residual water from the reaction media. To purify these, the crude material was dissolved in CH₂Cl₂ and dried over Na₂SO₄.

Table 2. Preparation of tetrafluoroborates **2a–h** by anion exchange.^[a]



Product	Yield [%]	Product	Yield [%]
2a	94	2e	91
2b	94	2f	86
2c	92	2g	86
2d	95	2h	87

[a] Reaction conditions: Amidinium bromide **1a–h** (1.0 mmol) in acetone (100 mL), NaBF₄ (660 mg, 6.0 equiv) in water (75 mL), r.t., 45 min.

An inspection into the ¹H NMR and ¹³C{¹H} NMR signals of amidinium salts **1a–h** and **2a–h** offers relevant information about these new class of NHC pro-ligands (Table 3). On the one hand, a trend in highfield shift of the amidinium-proton resonance is observed when increasing the heterocycle ring size from nine (8.17–8.54 ppm) to ten (7.26–7.73 ppm). This implies that the amidinium proton in the ten-membered ring NHC salts is less acidic than the corresponding proton in the nine-membered analogues, which is in agreement with previous observations made by Cavell and co-workers for six- and seven-membered ring NHC salts.^[10,12h,13c] On the other hand, a similar trend is noted in the carbon resonance whose ¹³C{¹H} NMR signals reveal an upfield shift when the heterocycle ring size increases from nine (164.2–165.6 ppm) to ten (156.9–157.7 ppm).

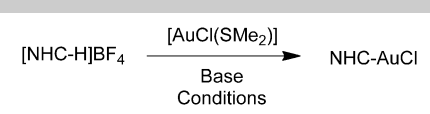
Table 3. ¹H and ¹³C{¹H} NMR shifts [ppm] of NHC–HX salts **1a–h** and **2a–h**.^[a]

Substrate	¹ H NMR N–CH–C [ppm]		¹³ C{ ¹ H} NMR [ppm]	
	1 X = Br [−]	2 X = BF ₄ [−]	1 X = Br [−]	2 X = BF ₄ [−]
[(9-Mes)H] ⁺	a 8.45	7.81	165.6	165.0
[(10-Mes)H] ⁺	e 7.26	7.25	157.7	157.9
[(9-Dipp)H] ⁺	b 8.46 ^b	7.91 ^b	164.4	163.6
[(10-Dipp)H] ⁺	f 7.40	7.46 ^d	156.9	157.4
[(9-Xyl)H] ⁺	c 8.54	8.03	165.5	165.7
[(10-Xyl)H] ⁺	g 7.29	7.30	157.4	157.6
[(9-Dietph)H] ⁺	d 8.17 ^c	7.84 ^c	164.2	164.1
[(10-Dietph)H] ⁺	h 7.73	7.29	157.3	157.5

[a] Values are given in ppm. Unless other stated, values were determined in CDCl₃ at 400 MHz (¹H) and 101 MHz (¹³C{¹H}). [b] Determined in CDCl₃ at 500 MHz (¹H) and 126 MHz (¹³C{¹H}). [c] Determined in CDCl₃ at 600 MHz (¹H) and 151 MHz (¹³C{¹H}). [d] Determined in CD₂Cl₂.

Finally, the anion exchange was also confirmed by ¹H NMR. The signals of compounds **2a–d** are notably displaced upfield (7.25–8.03 ppm) relative to their precursors **1a–d** Table 4(7.26–8.54 ppm) which also is an evidence of the diminished acidity

Table 4. Screening of conditions for the synthesis of NHC-gold(I) complexes.



Entry	Substrate	Base	Conditions ^[a,b]	Yield [%] ^[c]
1	2a	LiHMDS ^[d]	−40 °C	traces
2	2a	LiHMDS	−78 °C	traces
3	2a	KHMDS	−40 °C	traces
4	2b	KHMDS	−78 °C	12
5	2b	NaHMDS ^[d]	−78 °C	traces
6	2f	KHMDS	−78 °C	N.R
7	2e	LiHMDS	−78 °C	N.R
8	2e	KHMDS	−78 °C	traces
9	2b	MeONa	0 °C	N.R
10	2b	NaH	0 °C	N.R
11	2b	NaH	0 °C, tBuOK 10 mol %	8
12	2f	NaH	0 °C, tBuOK 10 mol %	traces
13	2b	tBuOK	0 °C	15
14	2b	tBuONa ^[e]	0 °C	10
15	2b	tBuONa ^[e]	−40 °C	19
16	2b	tBuOK	−40 °C	21
17	2b	tBuOK	−78 °C	31
18	2a	tBuOK ^[d]	−40 °C	27
19	2a	tBuOK ^[d]	−78 °C	42
20	2f	tBuOK ^[d]	−78 °C	38
21	2f	Et ₃ N	0 °C, DCM, open air	N.R
22	2b	K ₂ CO ₃	60 °C, acetone, open air	N.R
23	2f	K ₂ CO ₃	60 °C, acetone, open air	N.R

[a] Reaction conditions: tetrafluoroborate salt (0.1 mmol, 1.0 equiv), [AuCl(SMe₂)] (0.1 mmol, 1.0 equiv), Base (1.0 equiv), THF (10 mL); excluding Et₃N, all bases were employed as solids directly from the containing bottle. [b] Unless other stated, reactions were carried out under an inert atmosphere of N₂ using dry THF. [c] Yields of isolated materials are reported. [d] 1.0 M in dry THF (commercially available) was employed. [e] 2.0 M in dry THF (commercially available) was employed.

of the amidinium proton. Displacement of proton resonance is almost unnoticeable in **2e** and **2g** (< 0.01 ppm). The signals of the amidinium carbon are essentially unaltered after anion exchange (< 0.3 ppm).

Single crystals suitable for X-ray crystal structure analysis of **1b**, **1c**, **1f**, and **1g** were obtained by slow diffusion of hexane into concentrated solutions of the compound in CH₂Cl₂ or CHCl₃, followed by evaporation of solvents at room temperature, typically after one day. The solid-state structures show a wide N-CH-N angle (127.2–134.5°) (Figure 2).^[17]

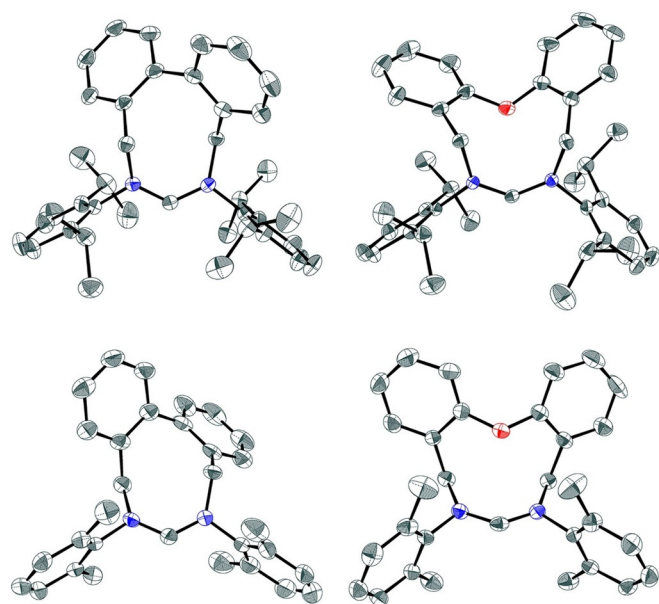


Figure 2. Molecular structure (ORTEP representation) of bromides **1b** (top left), **1f** (top right), **1c** (bottom left), and **1g** (bottom right) in the solid state. Thermal ellipsoids are shown at 50% probability level. Bromide anions and all hydrogen atoms have been omitted for clarity.

NHC-gold(I) complexes

Despite several attempts employing various reaction conditions, efforts to isolate the free carbene species were unsuccessful.^[18] Instead, a mixture of starting material and/or decomposition products were observed by NMR analysis of the resulting solids or the crude reaction mixtures. To circumvent these problems, we investigated the reaction of tetrafluoroborate salts in situ deprotonation in presence of AuCl(SMe₂), as the method to directly access the NHC-gold(I) complexes (Table 4).

The treatment of selected substrates with recurrently employed bis(trimethylsilyl)amides (e.g. NaHMDS, LiHMDS) gave only traces of product as judged by TLC (Table 4, entries 1–3, 5, 8). Interestingly, small quantities of the desired gold(I) complex were isolated when (9-Dipp)HBF₄ (**2b**, Dipp: 2,6-diisopropylphenyl) reacted with KHMDS (entry 4). Other examined bases (MeONa, NaH, Et₃N, K₂CO₃) were unable to deprotonate to the substrate under the explored conditions (entries 9, 10, 21, and 22) instead, a purple to dark solid corresponding to colloidal gold, appeared.

When *t*BuOK was employed as an additive to NaH (Table 4, entry 11), isolable quantities of gold(I) complex **2b** (8%) were

obtained. An equivalent quantity of *t*BuOK gave 15% when used under same conditions (entry 13). The experiment at –40 °C increased the yield to 21% (entry 16) whereas the reaction at –78 °C yielded 31% of the gold(I) complex (entry 17). The employment of a solution of *t*BuONa also showed a promising result (19% yield, entry 15) relative to that using solid *t*BuOK under same conditions (21% yield, entry 16). When using a solution of *t*BuOK, 27% yield at –40 °C (entry 18) and 42% yield at –78 °C (entry 19), were achieved. These preliminary observations indicated that an environment free of possible contaminants (water, KOH or *t*BuOH), as well as temperature below –40 °C, are optimal factors for the generation and stability of the carbene in the reaction media, and thus, determine the NHC-gold(I) formation. With this set of experiments, we partially concluded that *t*BuOK is a feasible deprotonating agent for the current NHC salts **2a–h**.

Table 5. Optimization of the synthesis of NHC-AuCl complexes.

$\begin{array}{ccc} & [\text{AuCl}(\text{SMe}_2)] (0.1 \text{ mmol}) \\ & \xrightarrow{\text{tBuOK} (0.1 \text{ mmol})} & \mathbf{3} \\ \mathbf{2a} & & \\ (0.1 \text{ mmol}) & \xrightarrow[\text{THF} (5 \text{ mL})]{-78^\circ\text{C to r.t., 18 h.}} & \end{array}$		
Entry	Variation of the stated conditions	Yield [%] ^[a]
1	none	35
2	–40 °C to r.t., 0.2 mmol <i>t</i> BuOK	28
3	0.20 mmol <i>t</i> BuOK	44
4	0.30 mmol <i>t</i> BuOK	45
5	0.15 mmol 2a , 0.20 mmol <i>t</i> BuOK	52
6	0.20 mmol 2a , 0.20 mmol <i>t</i> BuOK ^[b]	58
7	0.20 mmol 2a , 0.30 mmol <i>t</i> BuOK ^[b]	67
8	0.20 mmol 2a , 0.30 mmol <i>t</i> BuOK, 40 mg 4 Å MS (additive)	65

[a] Yields of isolated material. [b] 1.0 M in dry THF (commercially available) was employed. MS: molecular sieves.

The original conditions afforded 35% of complex **3** (Table 5, entry 1). When the quantity of *t*BuOK was doubled and temperature lowered to –40 °C, the yield dropped to 28% (entry 2). A slight improvement was observed when maintaining the initial temperature at –78 °C and using 0.20 mmol of base (44% yield, entry 3). Increasing the ratio of *t*BuOK (0.3 mmol, 3.0 equiv, entry 4), did not considerably impact on the yield (45%). Increasing the quantity of substrate **2a** to 0.15 mmol in the presence of 0.20 mmol *t*BuOK gave a comparatively good result (52%, entry 5). A slight rise in the yield was achieved (58%) when employing 0.20 mmol of both substrate **2a** and *t*BuOK in solution (entry 6). Furthermore, increasing the quantity of *t*BuOK to 0.30 mmol, led to an improved yield (67%, entry 7). Moreover, with the employment of solid *t*BuOK and freshly activated 4 Å molecular sieves as an additive, the reaction also occurred in good yield (65%, entry 8). Thus, the reaction conditions presented in the entries 7 and 8 (Table 5) seemed to be the optimal for the synthesis of further examples of NHC-gold(I) complexes using the salts **2a–h**. To

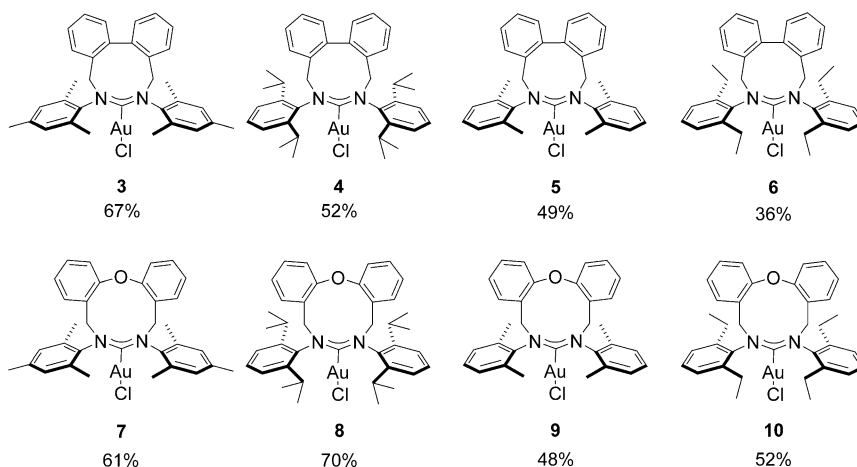


Figure 3. First examples of nine- and ten-membered-ring NHC-gold(I) complexes.

our delight, the representative series of gold(I) complexes **3–10**, bearing the newly developed NHC ligands, were successfully synthesized (Figure 3).

Regardless of the inert conditions and the use of degassed solvent or molecular sieves as additive, the workup procedure was performed under open-air conditions at room temperature because the gold(I) complexes are very stable solids. Through this straightforward approach, the direct complexation of the gold(I) with the free carbene in solution led to the desired NHC-gold(I) complexes in good yields and purity, making the overall synthesis a one-step process instead of the classical procedure (isolation of the free carbene and subsequent reaction with a metal source).^[6b]

Analysis of the compounds by ¹H NMR spectroscopy reveals the disappearance of the characteristic amidinium proton between 7.29–8.03 ppm in accordance with gold(I)-complex formation. In the ¹³C NMR spectra, the chemical shifts for the carbene carbon atoms (N–C_{NHC}–N) are found between 208.9–214.8 ppm (Table 6). These values are significantly lowfield shifted (≈ 50 ppm) compared with the amidinium carbon peak (N–CH–N) of the starting precursors (¹³C{¹H} NMR signals: 157.4–165.7 ppm, Table 2), which confirms the complex forma-

tion. This new series of NHC-gold(I) complexes show a N–C_{NHC}–N signal evidently less shielded by more than $\Delta\delta = 7$ ppm in the spectra, when compared with the examples reported in the literature (Table 6, entries 1–5). ¹³C{¹H} NMR signals of nine-membered NHC complexes (211.7–214.8 ppm) are slightly more deshielded than the ten-membered ones (208.9–210.3 ppm).

The structures of complexes **3**, **4**, **6**, and **7** were confirmed by X-ray crystallography (Table 7). Single crystals were grown by layering pentane on a solution of the gold(I) complex at room temperature followed by slow evaporation of solvents. The crystal structures do not show any aurophilic interactions (Au–Au) and were found to adopt a relative common spatial conformation. An inspection of the angles and bond lengths revealed some insightful characteristics. As can be seen from Table 7, the four complexes show the two-coordinated gold(I) atom in a nearly linear arrangement, with C_{NHC}–Au–Cl bond angles close to 180° (175.39(7)–179.46(8)°). The C_{NHC}–Au bond lengths range from 1.991(6) to 2.007(6) Å and fall within the range of previously reported values found in other essentially comparable compounds such as Au(7-Dipp)Cl (2.01),^[11a] Au(6-Dipp)Cl (2.01),^[14] Au(6-Mes)Cl (1.99),^[11a] or Au(IPr)Cl (1.94 Å).^[19]

A notable change is the decrease in the N–C_{NHC}–N angle upon coordination of the NHC ligand. For instance, the N–CH–N angle of amidinium bromide **1b** changes from 127.1(3)° to 117.2(5)° in the gold(I) complex **4**. The widest angle is observed in the ten-membered-ring complex **7** (119.5(2)°) which is about 0.9° larger than that of complexes **3** and **6** (with angles 118.6(2) and 118.6(5)°) and approximately 2.3° larger than that of complex **4** (117.2(5)°), that possess a nine-membered NHC ligand. If compared with other NHC-gold(I) complexes found in literature, the N–C_{NHC}–N angles of **3**, **4**, and **6** are evidently larger than those in Au(IPr)Cl (102.4°)^[19] and Au(I-Mes)Cl (107.0°),^[21] but similar to those of the six-membered counterparts Au(6-Dipp)Cl (119.0°)^[14] and Au(6-Mes)Cl (118.6°).^[11a] To our surprise, the major difference in the structures of complexes **3**, **4**, **6**, and **7** is that the N–C_{NHC}–N angles are significantly smaller than those found in complex Au(7-Dipp)Cl (121.2°).^[11a]

Table 6. ¹³C NMR displacement shifts of carbene carbon (N–C_{NHC}–N) in complexes **3–10** and selected examples found in the literature.

Entry	Complex	Reference	C _{NHC} [ppm]
1	Au(IPr)Cl	Ref. [19]	175.9
2	Au(6-Mes)Cl	Ref. [11a]	192.6
3	Au(7-Dipp)Cl	Ref. [11a]	193.1
4	Au(6-Dipp)Cl	Ref. [14]	200.9
5	Au(7-Dietph)Cl	Ref. [13a]	201.7
6	Au(9-Mes)Cl	3 This work	211.9
7	Au(9-Dipp)Cl	4 This work	212.6
8	Au(9-Xyl)Cl	5 This work	214.8
9	Au(9-Dietph)Cl	6 This work	211.7
10	Au(10-Mes)Cl	7 This work	209.3
11	Au(10-Dipp)Cl	8 This work	210.3
12	Au(10-Xyl)Cl	9 This work	208.9
13	Au(10-Dietph)Cl	10 This work	209.9

Compound	X-ray structure ^[a]	Topographic Steric Map	Selected parameters
3			$C_{\text{NHC}}-\text{Au}$ 1.992(2) Å $\text{Au}-\text{Cl}$ 2.2865(6) Å $\angle C_{\text{NHC}}-\text{Au}-\text{Cl}$ 179.46(8)° $\angle \text{N}-\text{C}_{\text{NHC}}-\text{N}$ 118.6(2)° $\angle \alpha$ 39.3° $\%V_{\text{bur}}$ 43.6
4 ^[b]			$C_{\text{NHC}}-\text{Au}$ 1.991(6) Å $\text{Au}-\text{Cl}$ 2.3050(14) Å $\angle C_{\text{NHC}}-\text{Au}-\text{Cl}$ 177.64(16)° $\angle \text{N}-\text{C}_{\text{NHC}}-\text{N}$ 117.2(5)° $\angle \alpha$ 48.2° $\%V_{\text{bur}}$ 53.0
6			$C_{\text{NHC}}-\text{Au}$ 2.007(6) Å $\text{Au}-\text{Cl}$ 2.354(14) Å $\angle C_{\text{NHC}}-\text{Au}-\text{Cl}$ 176.81(17)° $\angle \text{N}-\text{C}_{\text{NHC}}-\text{N}$ 118.6(5)° $\angle \alpha$ 53.6° $\%V_{\text{bur}}$ 48.4
7			$C_{\text{NHC}}-\text{Au}$ 1.997(3) Å $\text{Au}-\text{Cl}$ 2.2845(7) Å $\angle C_{\text{NHC}}-\text{Au}-\text{Cl}$ 175.39(7)° $\angle \text{N}-\text{C}_{\text{NHC}}-\text{N}$ 119.5(2)° $\angle \alpha$ 52.4° $\%V_{\text{bur}}$ 43.6

[a] Ellipsoids are shown at 50% probability level with all hydrogen atoms and solvent molecules omitted for clarity. [b] Only one of the two symmetry-independent molecules in the unit cell is shown for clarity.

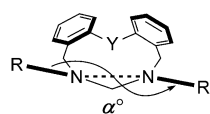


Figure 4. Torsional angle α° in expanded-ring NHC complexes.

The torsional angle α° between the planes, defined by the $C_{\text{Ar}}-\text{N}\cdots\text{N}-C_{\text{Ar}}$ atoms (Figure 4), was introduced by Iglesias et al.^[1c,12j] as a measurement of the spatial twist and the relative position of the aromatic substituents, which point into the metal's coordination sphere. The torsional angle α found in

complex **3** is 39.3° whereas in **7** it is 52.4°. Complex **6** exhibits the most pronounced twisting ($\alpha=53.6^\circ$). The relative orientation of aryl substituents in **4** ($\alpha=48.2^\circ$) places one of the isopropyl groups of each aryl substituent slightly away from the metal center.

A closer inspection of the biphenyl and diphenyl ether backbones offered some interesting characteristics. In **7** the angle $C_{\text{Ar}}-\text{O}-C_{\text{Ar}'}$ is 120.2°, whereas the angle between the phenyl ring

planes PL1 and PL2, is 69.9° (with PL1 = C1_{Ar}...C6_{Ar} and PL2 = C1_{Ar}...C6_{Ar}). This value is smaller than that observed by least-squares in either of the two crystallized forms of diphenyl ether molecule that showed angles of 87.6–88.4° between the phenyl ring planes PL1 and PL2^[22] indicating a highly strained conformation, upon NHC formation. Torsion angles, formed by intersection of the two aryl planes in the backbone of complexes **3**, **4**, and **6**, were found to be 54.6°, 48.7°, and 57.0°, respectively.

The percent of buried volume (%V_{bur})^[23] and topographic steric map (TSM)^[20,24] have emerged as molecular descriptors of the spatial distribution of steric bulk in N-heterocyclic carbenes. Using the method developed by Cavallo,^[25] we have derived topographic steric maps and %V_{bur} values for the ligands (Table 7). As expected, complex **4**, possessing diisopropylphenyl substituents at the nitrogen atoms, is the most sterically hindered example (%V_{bur} 53.0). Nonetheless, its TSM reveals some unfilled space and a heterogeneous steric distribution. Complexes **3** and **7** exhibit the same %V_{bur} values (43.6) and share a basically identical steric distribution around the metal atom. Complex **6** shows a slightly higher %V_{bur} value (48.4) but its TSM showed a non-uniform steric distribution towards the gold(I) center. To gain insight into the steric characteristics of the present gold(I) complexes, we made a brief comparison with other related NHC complexes bearing expanded-ring cores and bulkier ligands (Table 8).

Entry	Complex	Reference	%V _{bur}
1	Au(6-Mes)Cl	Ref. [11a]	42.2
2	Au(7-Dietph)Cl	Ref. [13a]	43.3
3	Au(9-Mes)Cl 3	This work	43.6
4	Au(10-Mes)Cl 7	This work	43.3
5	Au(IPr)Cl	Ref. [19]	45.6
6	Au(Dietph)Cl 6	This work	48.4
7	Au(IPent)Cl	Ref. [26]	49.4
8	Au(IPr*)Cl	Ref. [27]	50.4
9	Au(6-Dipp)Cl	Ref. [14]	50.8
10	Au(INon)Cl	Ref. [28]	51.3
11	Au(IHept)Cl	Ref. [28]	51.5
12	Au(7-Dipp)Cl	Ref. [11a]	52.6
13	Au(9-Dipp)Cl 4	This work	53.0

[a] %V_{bur} values were taken directly as reported or from CIF files available in CCDC using SambVca 2.0.^[25a,c]

Notably, the five-membered NHC-gold(I) complexes bearing the bulky IPr (1,3-bis(2,6-diisopropylphenyl)imidazole-2-ylidene), IPent (1,3-bis(2,6-di-3-pentylphenyl)imidazol-2-ylidene) and IPr* (1,3-bis(2,6-bis(diphenylmethyl)-4-methylphenyl)imidazol-2-ylidene) (Table 8, entries 5, 7 and 8) possess higher %V_{bur} values (45.6–50.4) than complexes **3** and **7** (entries 3 and 4), both with a %V_{bur} value of 43.6. Moreover, they all are still smaller than those complexes with 6-Dipp and 7-Dipp ligands with %V_{bur} values of 50.8 and 51.6 respectively (entries 9 and 10). To the best of our knowledge, the complex **4** has the larg-

est %V_{bur} value of any expanded-ring NHC-AuCl complex reported to date, surpassing the %V_{bur} 52.6 of Au(7-Dipp)Cl reported by Dunsford et al.^[11a] (entry 12).

Although the alkyl-chain-containing cores of six- to eight-membered-ring NHC ligands can adopt flexible conformations which lead to less predictable features,^[11a] the presence of a relatively rigid biphenyl and diphenyl ether moieties at the backbone ring, can contribute to the structural stability of the metal complexes. This pattern also might establish certain limits for the construction of larger and rigid ring systems of similar nature (i.e. eleven-membered NHC ligands).

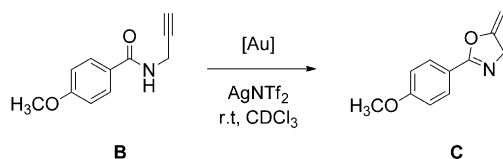
In general, the metal complexes **3–10** are easy to purify by recrystallization. The solids are stable in open air conditions at room temperature and can be stored indefinitely in a freezer. The melting points of these species lie around 300 °C. All the complexes are stable in CDCl₃ or CD₂Cl₂ solutions at room temperature, but decomposition might be observed on storage (> 6 weeks). Solutions of the complexes (≈ 0.1 M) in wet solvents (CH₂Cl₂ or THF) can be preserved at low temperatures (below 4 °C) for several weeks, but if kept on the bench at room temperature, colloidal gold (purple-dark), might appear. We have found the complexes to be resilient to chromatographic purification (SiO₂) with no significant loss of yield (< 7%).

First study of the catalytic activity of NHC-gold(I) complexes

Given the continuously growing field of catalyzed reactions using expanded-ring NHC-gold(I) complexes,^[29] we selected the gold(I)-catalyzed oxazole synthesis^[30] as a benchmark reaction for the assessment of the catalytic activity of the gold(I) complexes **3–10**. Thus, 4-Methoxy-N-(2-propyn-1-yl)benzamide **B**, acted as a model substrate and initially 1.0 mol% pre-catalyst loading was investigated in the presence of AgNTf₂ employed as the chloride scavenger (Table 9).

Employing 1.0 mol% catalyst loading, a 99% yield was observed for complexes **3**, **5**, **6**, **7**, and **9** (Table 9, entries 2, 9, 13, 16, and 24) after 24 hours of reaction. Complex **10** reached 90% yield (entry 28) and **8** gave the product in 44% yield (entry 20) at the same reaction time. Although complex **4** needed 24 hours (entry 6), complexes **3**, **5**, and **9** required only 3 hours to reach almost 50% yield (entries 1, 8, and 23). Interestingly, catalysts **6** and **7** surpassed 60% yield after 3 hours (entries 12 and 15) and complexes **5**, **8** and **10** achieved 17–42% yield, at same reaction time (3 h, entries 5, 19, and 27). Outstandingly, after 72 hours of reaction, complex **3** offered 98% yield at 0.3 mol% loading (entry 4) whereas complex **5** reached 91% yield at 0.15 mol% loading (entry 10). We then reduced catalyst loadings to 0.1 mol%. Complex **3** furnished 82% yield (entry 3) and complexes **7**, **9**, and **10**, passed the 50% mark (entries 17, 25, and 29), after 48 hours. Catalyst **5** and **8** showed a lower catalytic activity (< 33%, entries 11 and 21). Despite the need for longer times (> 5 days), good yields were still observed for **4** (92%, entry 7), **8** (85%, entry 22), **9** (100%, entry 26), and **10** (96%, entry 30). Complex **6** showed a slow activity through the days (6 days, 20%, entry 14). At 0.05 mol% loading, complex **7** afforded 24% yield after 6 days (entry 18).

Table 9. NHC-gold(I)-catalyzed cycloisomerization of propargylamide.



Entry	[Au] complex	Conditions ^[a]	Yield (%) ^[b]
1	3	1.0 mol%, 3 h	47
2	3	1.0 mol%, 24 h	100
3	3	0.1 mol%, 48 h	82
4	3	0.3 mol%, 72 h	98
5	4	1.0 mol%, 3 h	21
6	4	1.0 mol%, 24 h	50
7	4	0.1 mol%, 5 d	92
8	5	1.0 mol%, 3 h	48
9	5	1.0 mol%, 24 h	99
10	5	0.15 mol%, 72 h ^[c]	91
11	5	0.10 mol%, 48 h	33
12	6	1.0 mol%, 3 h	61
13	6	1.0 mol%, 24 h	100
14	6	0.1 mol%, 6 d ^[c]	20
15	7	1.0 mol%, 3 h	60
16	7	1.0 mol%, 24 h	100
17	7	0.1 mol%, 48 h ^[c]	69
18	7	0.05 mol%, 6 d	24
19	8	1.0 mol%, 3 h	17
20	8	1.0 mol%, 24 h	44
21	8	0.1 mol%, 48 h	31
22	8	0.1 mol%, 6 d	85
23	9	1.0 mol%, 3 h	49
24	9	1.0 mol%, 24 h	99
25	9	0.1 mol%, 48 h	51
26	9	0.1 mol%, 6 d	100
27	10	1.0 mol%, 3 h	42
28	10	1.0 mol%, 24 h	90
29	10	1.0 mol%, 48 h	50
30	10	0.1 mol%, 6 d	96

[a] Reactions were carried out at room temperature at 100 μ mol scale in CDCl₃ (500 μ L). [b] Determined by ¹H NMR as an average of two runs, using hexamethylbenzene as internal standard. [c] Carried out in CD₂Cl₂.

We next investigated whether the scope with regard to the gold(I) complexes could be improved by heating (Table 10). Total reaction time was 24 hours and the temperature was 50 °C. Thus, a 91% conversion was achieved with 0.05 mol% of **3** (entry 1), whereas a 60% yield was observed when loading was reduced to 0.025 mol% (entry 2). Complexes **8** and **9** reached 14% and 15% yield under the same conditions (entries 8 and 9) whereas only 7% yield was observed for catalyst **10** (entry 10). As expected from the prior experiments, complex **3** proved to be a very active catalyst at a 0.005 mol% loading, affording 19% yield which corresponds to a TON = 3800 (entry 3). The more sterically encumbered complex **4** gave only 6% yield employing five times more of catalyst (0.025 mol%, entry 4). Despite the heating conditions, a 0.025 mol% loading of complexes **5**, **6**, and **7** proved insufficient for effecting cycloisomerization (< 11% yield, entries 5–7).

Previous studies on this cycloisomerization reaction have shown 95% yield in 12 hours using 5 mol% of AuCl₃^[30a] or 79% after 36 hours, employing a lower catalyst loading of a phosphine-based complex (1.0 mol% (Ph₃P)AuNTf₂)^[31] Recent-

Table 10. NHC-gold(I)-catalyzed cycloisomerization of **B** under heating.^[a]

Entry	[Au] complex	Pre-catalyst loading [mol%]	Yield [%] ^[b]	TON
1	3	0.050	91	1820
2	3	0.025	60	2400
3	3	0.005	19	3800
4	4	0.025	6	240
5	5	0.025	11	440
6	6	0.025	10	400
7	7	0.025	11	440
8	8	0.025	14	560
9	9	0.025	15	600
10	10	0.025	7	280

[a] Reactions were carried out at 200 μ mol scale in CHCl₃ (2.0 mL). [b] Determined by GC-MS using dodecane as internal standard.

ly, some examples of HAAC (Hydrazino amino acyclic carbene) complexes were developed in our group, that gave up to 100% yield, but at the expense of a prolonged reaction time (2 days).^[32]

If we consider the steric characteristics of the complexes **3**, **4**, **6**, and **7**, we can assess a closer relationship with their catalytic activity. Under exactly the same experimental conditions (1.0 mol% catalyst, 24 h, room temperature), complex **4** (%V_{bur} 53.0) afforded 50% conversion, whereas complexes **3** (%V_{bur} 43.6), **6** (%V_{bur} 48.4), and **7** (%V_{bur} 43.6) achieved 99–100% conversion. The steric maps also support these results; in complexes **3**, **6**, and **7** the steric hindrance around the metal atom seems to be more homogeneously distributed, despite some uncovered field, in a difference to **4**, in which two quadrants appear to be bulkier, whereas the other two show a lower steric hindrance; in other words, only two of the four isopropyl groups of the aryl substituents are pointing toward the metal atom and the remaining two have a negligible steric influence in the metal's coordination sphere. The observed distortion between (N-attached) aryl planes **4** ($\alpha = 49.2^\circ$) irrevocably confirms this postulate, in contrast to **3** ($\alpha = 39.3^\circ$) in which the four methyl substituents of the aryls are pointing towards the gold center in a relative uniform manner. This steric distribution might explain the high catalytic activity of complex **3** in the given reaction.

Overall, we have shown that a sterically well-distributed ligand can deliver a better catalytic activity than a sterically bulkier one, confirming certain limits on the *larger is more efficient* concept,^[33] particularly when designing expanded-ring NHC ligands.

Conclusions

The development of amidinium bromides **1 a–h** as NHC pro-ligands, is reported for the first time. The synthesis of gold(I) complexes **3–10** is accomplished by in situ proton abstraction of tetrafluoroborates **2 a–h**, with tBuOK in the presence of AuCl(SMe₂) in acceptable yields (36–70%). Solid-state structures of NHC-gold(I) complexes **3**, **4**, **6**, and **7** revealed N-C_{NHC}-N angles in the range 118.61–119.48°, and a similar spatial con-

formation. Calculated % V_{bur} values lie between 43.6–53.0, with Au(9-Dipp)Cl **4** (% V_{bur} 53.0) being the sterically most hindered. Gold(I) complexes **3**, **5**, **6**, **7**, and **9** exhibited exceptional catalytic activity in a selected cycloisomerization reaction (1.0 mol%, up to 100% conversion). Importantly, heating conditions can help shorten reaction times without decreasing the catalyst performance (**3**, 0.05 mol%, up to 91% conversion). The most effective gold(I) species of the tested for catalysis was **3** at relatively low loadings (0.05–0.025 mol%), followed by **7**, **9**, and **10** at 0.1 mol% loadings. Furthermore, gold(I) catalysis imparted for these complexes can be performed in air, under open-flask conditions or prolonged reaction times without detrimental effects. Owing to this exceptional performance, the present gold(I) complexes have the potential to be tremendously useful in gold(I) catalyzed reactions.

Experimental Section

General considerations

NMR characterization data was collected at 296 K (unless otherwise stated) at the Department of Chemistry of the University of Heidelberg on Bruker Avance DRX 300 (300 MHz), Bruker Avance III 400 (400 MHz), Bruker Avance III 500 (500 MHz), and Bruker Avance III 600 (600 MHz). The chemical shifts in the ^1H and ^{13}C spectra are given relative to TMS (0.00 ppm) and referenced to the residual proton signal in deuterated solvents (CD_2Cl_2 : 5.22 ppm, 53.84 ppm; and CDCl_3 : 7.19 ppm, 77.16 ppm). Data for ^1H NMR are reported as follows: chemical shift δ are given in parts per million (ppm), multiplicity (s=singlet, d=doublet, t=triplet, q=quartet, m=multiplet, dd=double doublet, td=triple doublet, br s=broad singlet) and coupling constant J in Hz, integration. ^{13}C NMR spectra were measured with ^1H -decoupling. The multiplicities mentioned in these spectra [s (singlet, quaternary carbon), d (doublet, CH-group), t (triplet, CH_2 -group), q (quartet, CH_3 -group)] were determined with help of DEPT135, HSBC and HMQC experiments. Melting points were determined in a BÜCHI automated B-545 apparatus and are uncorrected. High resolution mass spectra (HRMS) were recorded on a Bruker Apex-Qe hybrid 9.4 FT-ICR spectrometer (ESI+, MALDI). IR spectra (in cm^{-1}) were recorded on a Bruker Vector 22 Lumos FT-IR. GC/MS spectra were measured using an Agilent 7890A gas chromatograph with an Agilent 5975C Series MSD mass analyzer and using helium as a carrier gas. UV/Vis were recorded in a V-670 UV-VIS-NIR Spectrophotometer. For the X-Ray diffraction analyses, the intensity data were collected at 200(2) K on Bruker Smart CCD or Bruker APEX-II diffractometers ($\text{Mo}_{\text{K}\alpha}$ radiation, $\lambda=0.71073 \text{ \AA}$). The structures were solved by direct methods with SHELXT-2014^[34] and refined by full-matrix least-squares procedures using the SHELXL-2017/1 software^[35] with anisotropic thermal parameters for all the non-hydrogen atoms. CCDC 1918016 (**1b**), 1918017 (**1c**), 1918018 (**1f**), 1918019 (**1g**), 1918020 (**3**), 1918021 (**4**), 1918022 (**6**), and 1918023 (**7**) contain the supplementary crystallographic data for this paper. These data are provided free of charge by The Cambridge Crystallographic Data Centre

General procedure for the synthesis of amidinium bromides

1a–h

To a stirred solution of N,N' -diarylformamidinium (1.0 mmol) in CH_3CN (400 mL) was added finely grinded K_2CO_3 (1.0 mmol, 1.0 equiv) and mixture was stirred for 45 min at room temperature. Then, the corresponding dibromoalkane (1.1 mmol, 1.1 equiv) was added to the

suspension in one portion, and the mixture was stirred 24 hours at same temperature after which it was heated to 85 °C for 3–4 days until full consumption of the dibromoalkane (monitored by TLC). The suspension was cooled down to room temperature and filtered. The solvent was removed under reduced pressure, CH_2Cl_2 (100 mL) was added and solids were filtered off. The filtrate was evaporated until dryness to give a solid which was recrystallized from toluene/ n -hexane to give amidinium bromides as white or yellowish solids.

1a: Colorless solid; yield: 367 mg. (68%); m.p: 239–240 °C; ^1H NMR (400 MHz, CDCl_3): $\delta=8.45$ (s, 1H), 7.57–7.46 (m, 2H), 7.37 (t, $J=7.0$ Hz, 4H), 7.05 (d, $J=7.4$ Hz, 2H), 7.01 (d, $J=7.2$ Hz, 4H), 5.05 (d, $J=14.7$ Hz, 2H), 4.70 (d, $J=14.7$ Hz, 2H), 2.30 (s, 6H), 2.28 (s, 6H), 2.20 ppm (s, 6H); ^{13}C NMR (101 MHz, CDCl_3): $\delta=165.60$ (d, 1C), 141.20 (s, 2C), 139.66 (s, 2C), 137.94 (s, 2C), 135.82 (s, 2C), 133.08 (s, 2C), 132.64 (s, 2C), 131.66 (d, 2C), 131.41 (d, 2C), 130.85 (d, 2C), 130.50 (d, 2C), 129.61 (d, 2C), 129.26 (d, 2C), 59.61 (t, 2C), 21.22 (q, 2C), 19.27 (q, 2C), 18.45 ppm (q, 2C); IR (ATR): $\tilde{\nu}=3066, 2997, 2866, 2740, 1644, 1585, 1473, 1441, 1403, 1380, 1350, 1308, 1291, 1204, 1177, 1121, 1094, 1036, 997, 949, 913, 883, 852, 826, 793, 776, 776, 754, 658, 621 \text{ cm}^{-1}$; UV/Vis (CH_2Cl_2): λ_{max} (log ϵ)=272 nm (3.73); HR-MS (ESI+) m/z calcd for $\text{C}_{33}\text{H}_{35}\text{N}_2$ [M–Br] $^+$: 459.2795, found: 459.2795.

1b: Colorless solid; yield: 508 mg (81%); m.p: 169 °C; ^1H NMR (500 MHz, CDCl_3): $\delta=8.46$ (s, 1H), 7.54 (td, $J=7.6, 1.0$ Hz, 2H), 7.50 (t, $J=7.8$ Hz, 2H), 7.39 (dd, $J=7.7, 0.9$ Hz, 2H), 7.34 (td, $J=7.6, 1.2$ Hz, 2H), 7.31 (dd, $J=7.8, 1.3$ Hz, 2H), 7.27 (dd, $J=7.9, 1.3$ Hz, 2H), 6.89 (d, $J=7.6$ Hz, 2H), 5.16 (d, $J=14.6$ Hz, 2H), 4.65 (d, $J=14.6$ Hz, 2H), 2.74–2.62 (m, 4H), 1.27 (d, $J=6.7$ Hz, 6H), 1.23 (d, $J=6.6$ Hz, 6H), 1.18 ppm (d, $J=6.7$ Hz, 6H), 1.10 (d, $J=7.0$ Hz, 6H); ^{13}C NMR (126 MHz, CDCl_3): $\delta=164.35$ (d, 1C), 146.80 (s, 2C), 143.69 (s, 2C), 139.22 (s, 2C), 136.39 (s, 2C), 132.05 (d, 2C), 131.74 (d, 2C), 131.61 (s, 2C), 131.27 (d, 2C), 129.87 (d, 2C), 129.02 (d, 2C), 127.13 (d, 2C), 125.21 (d, 2C), 61.69 (t, 1C), 61.65 (t, 1C), 29.58 (d, 1C), 29.54 (d, 1C), 29.14 (d, 1C), 29.10 (d, 1C), 27.04 (q, 1C), 27.00 (q, 1C), 25.56 (q, 1C), 25.51 (q, 1C), 25.39 (q, 1C), 25.34 (q, 1C), 22.62 (q, 1C), 22.57 ppm (q, 1C); IR (ATR): $\tilde{\nu}=3064, 3026, 2956, 2927, 2865, 2814, 2754, 2704, 2104, 1735, 1624, 1585, 1440, 1405, 1385, 1364, 1347, 1324, 1302, 1289, 1270, 1256, 1236, 1202, 1172, 1127, 1101, 1055, 1001, 953, 933, 920, 853, 800, 781, 752, 666, 632 \text{ cm}^{-1}$; UV/Vis (CH_2Cl_2): λ_{max} (log ϵ)=275 (3.77), 348 nm (3.38); HR-MS (ESI+) m/z calcd for $\text{C}_{39}\text{H}_{47}\text{N}_2$ [M–Br] $^+$: 543.3734, found: 543.3743.

1c: Colorless solid; yield: 498 mg; (72%). m.p: 229–230 °C; ^1H NMR (500 MHz, CDCl_3): $\delta=8.54$ (s, 1H), 7.52 (t, $J=7.6$ Hz, 2H), 7.38 (t, $J=7.2$ Hz, 4H), 7.31 (t, $J=7.6$ Hz, 2H), 7.22 (t, $J=6.6$ Hz, 4H), 7.04 (d, $J=7.5$ Hz, 2H), 5.08 (d, $J=14.7$ Hz, 2H), 4.75 (d, $J=14.7$ Hz, 2H), 2.35 (s, 6H), 2.26 ppm (s, 6H); ^{13}C NMR (126 MHz, CDCl_3): $\delta=165.45$ (d, 1C), 140.24 (s, 2C), 139.51 (s, 2C), 136.00 (s, 2C), 132.95 (s, 2C), 132.81 (s, 2C), 131.35 (d, 2C), 130.95 (d, 2C), 130.94 (d, 2C), 130.82 (d, 2C), 129.78 (d, 2C), 129.45 (d, 2C), 129.20 (d, 2C), 59.53 (t, 1C), 59.49 (t, 1C), 19.30 (q, 1C), 19.27 (q, 1C), 18.49 (q, 1C), 18.45 ppm (q, 1C); IR (ATR): $\tilde{\nu}=2982, 2951, 2917, 2859, 2830, 2774, 2739, 1735, 1633, 1584, 1469, 1441, 1399, 1344, 1396, 1295, 1204, 1156, 1122, 1092, 1033, 1006, 962, 948, 915, 892, 823, 801, 789, 770, 756, 731, 659, 618 \text{ cm}^{-1}$; UV/Vis (CH_2Cl_2): λ_{max} (log ϵ)=272 nm (3.84); HR-MS (ESI+) m/z calcd for $\text{C}_{31}\text{H}_{31}\text{N}_2$ [M–Br] $^+$: 431.2482, found: 431.2482.

1d: Pale brown solid; yield: 394 mg; (83%); m.p: 159–161 °C; ^1H NMR (600 MHz, CDCl_3): $\delta=8.17$ (s, 1H), 7.53 (td, $J=7.6, 1.1$ Hz, 2H), 7.45 (t, $J=7.8$ Hz, 2H), 7.39–7.33 (m, 4H), 7.29 (t, $J=8.1$ Hz, 4H), 6.99 (d, $J=7.7$ Hz, 2H), 5.13 (d, $J=14.7$ Hz, 2H), 4.70 (d, $J=14.7$ Hz, 2H), 2.67–2.55 (m, 4H), 2.54–2.44 (m, 4H), 1.23 (t, $J=7.5$ Hz, 6H), 1.19 ppm (t, $J=7.5$ Hz, 6H); ^{13}C NMR (151 MHz, CDCl_3):

$\delta = 164.24$ (d, 1C), 141.43 (s, 2C), 139.50 (s, 2C), 139.13 (s, 2C), 138.39 (s, 2C), 132.44 (s, 2C), 131.58 (d, 2C), 131.57 (d, 2C), 131.11 (d, 2C), 129.66 (d, 2C), 129.12 (d, 2C), 128.73 (d, 2C), 127.50 (d, 2C), 60.73 (t, 2C), 24.80 (t, 2C), 23.95 (t, 2C), 15.06 (q, 2C), 14.79 ppm (q, 2C); IR (ATR): $\tilde{\nu} = 2970, 2933, 2871, 1722, 1642, 1585, 1446, 1411, 1393, 1371, 1351, 1308, 1292, 1237, 1202, 1171, 1124, 1055, 1006, 955, 942, 913, 880, 853, 820, 784, 665, 627 \text{ cm}^{-1}$; UV/Vis (CH_2Cl_2): λ_{max} ($\log \epsilon$) = 277 (3.60), 355 nm (3.21); HR-MS (ESI+) m/z calcd for $\text{C}_{35}\text{H}_{39}\text{N}_2$ [M-Br] $^+$: 487.3108, found: 487.3109.

1e: colorless solid; yield: 264 mg (48%); m.p.: 199–200 °C; ^1H NMR (400 MHz, CDCl_3): $\delta = 7.58$ (d, $J = 7.8$ Hz, 2H), 7.36 (td, $J = 8.2, 1.7$ Hz, 2H), 7.26 (s, 1H), 7.00 (td, $J = 7.5, 0.8$ Hz, 2H), 6.91 (dd, $J = 7.5, 1.5$ Hz, 2H), 6.78 (s, 4H), 5.82 (s, 4H), 2.16 (s, 6H), 2.15 ppm (s, 12H); ^{13}C NMR (101 MHz, CDCl_3): $\delta = 157.74$ (d, 1C), 157.18 (s, 2C), 140.75 (s, 2C), 139.96 (s, 2C), 134.68 (s, 4C), 131.70 (d, 2C), 130.82 (d, 2C), 130.29 (d, 2C), 129.04 (d, 1C), 128.23 (d, 1C), 125.76 (d, 2C), 125.41 (s, 2C), 120.37 (d, 2C), 57.49 (t, 2C), 20.88 (q, 2C), 18.00 ppm (q, 4C); IR (ATR): $\tilde{\nu} = 3462, 3375, 2921, 2861, 2457, 1650, 1604, 1581, 1479, 1453, 1398, 1348, 1299, 1236, 1201, 1179, 1155, 1134, 1110, 1031, 987, 949, 877, 854, 791, 744, 702, 656, 637, 617 \text{ cm}^{-1}$; UV/Vis (CH_2Cl_2): λ_{max} ($\log \epsilon$) = 271 nm (3.64); HR-MS (ESI+) m/z calcd for $\text{C}_{33}\text{H}_{35}\text{N}_2\text{O}$ [M-Br] $^+$: 475.2744, found: 475.2746.

1f: Pale yellow solid; yield: 288 mg (45%); m.p.: 281 °C; ^1H NMR (400 MHz, CDCl_3): $\delta = 7.64$ (dd, $J = 8.2, 0.5$ Hz, 2H), 7.40 (s, 1H), 7.34 (td, $J = 8.2, 1.7$ Hz, 2H), 7.29 (t, $J = 7.8$ Hz, 2H), 7.10 (d, $J = 7.8$ Hz, 4H), 6.98 (td, $J = 7.5, 0.9$ Hz, 2H), 6.86 (dd, $J = 7.6, 1.5$ Hz, 2H), 5.95 (s, 4H), 3.45 (s, 4H), 1.10 (d, $J = 6.8$ Hz, 12H), 0.87 ppm (s, 12H); ^{13}C NMR (101 MHz, CDCl_3): $\delta = 157.74$ (s, 2C), 156.92 (d, 1C), 145.81 (s, 4C), 140.24 (s, 2C), 132.05 (d, 4C), 131.06 (d, 2C), 130.63 (d, 2C), 125.68 (d, 4C), 125.57 (s, 2C), 121.35 (d, 2C), 59.42 (t, 2C), 28.07 (d, 4C), 25.81 (q, 4C), 24.63 ppm (q, 4C); IR (ATR): $\tilde{\nu} = 3321, 2967, 2868, 2817, 1638, 1582, 1483, 1466, 1450, 1401, 1364, 1326, 1269, 1228, 1185, 1161, 1111, 1098, 1056, 990, 949, 933, 901, 849, 808, 792, 745, 701, 640, 615 \text{ cm}^{-1}$; UV/Vis (CH_2Cl_2): λ_{max} ($\log \epsilon$) = 271 nm (3.72); HR-MS (ESI+) m/z calcd for $\text{C}_{39}\text{H}_{47}\text{N}_2\text{O}$ [M-Br] $^+$: 559.3683, found: 559.3688.

1g: Colorless solid; yield: 255 mg (48%); m.p.: 200–202 °C; ^1H NMR (400 MHz, CDCl_3): $\delta = 7.59$ (d, $J = 7.8$ Hz, 2H), 7.36 (td, $J = 8.1, 1.7$ Hz, 2H), 7.29 (s, 1H), 7.14–7.07 (m, 2H), 6.99 (t, $J = 7.3$ Hz, 6H), 6.88 (dd, $J = 7.5, 1.5$ Hz, 2H), 5.85 (s, 4H), 2.20 ppm (s, 12H); ^{13}C NMR (101 MHz, CDCl_3): $\delta = 157.46$ (d, 1C), 157.14 (s, 2C), 142.97 (s, 2C), 135.06 (s, 4C), 131.65 (d, 2C), 130.91 (d, 2C), 129.97 (d, 2C), 129.76 (d, 4C), 125.60 (s, 2C), 125.44 (d, 2C), 120.38 (d, 2C), 57.59 (t, 2C), 18.10 ppm (q, 4C); IR (ATR): $\tilde{\nu} = 3377, 3010, 2884, 2827, 1650, 1584, 1482, 1450, 1234, 1188, 1164, 1112, 1095, 1034, 986, 950, 888, 847, 756, 701, 634 \text{ cm}^{-1}$; UV/Vis (CH_2Cl_2): λ_{max} ($\log \epsilon$) = 274 nm (3.63); HR-MS (ESI+) m/z calcd for $\text{C}_{31}\text{H}_{31}\text{N}_2\text{O}$ [M-Br] $^+$: 447.2431, found: 447.2434.

1h: Colorless solid; yield: 300 mg (51%); m.p.: 180 °C; ^1H NMR (400 MHz, CDCl_3): $\delta = 7.63$ (dd, $J = 8.2, 0.6$ Hz, 2H), 7.35 (td, $J = 8.0, 1.7$ Hz, 2H), 7.29 (s, 1H), 7.22 (t, $J = 7.7$ Hz, 2H), 7.05 (d, $J = 7.7$ Hz, 4H), 6.96 (td, $J = 7.5, 0.9$ Hz, 2H), 6.85 (dd, $J = 7.5, 1.6$ Hz, 2H), 5.86 (br s, 4H), 2.71–2.45 (m, 8H), 0.95 ppm (t, $J = 7.5$ Hz, 12H); ^{13}C NMR (101 MHz, CDCl_3): $\delta = 157.32$ (d, 1C), 157.22 (s, 2C), 141.63 (s, 2C), 140.65 (s, 4C), 131.94 (d, 2C), 130.99 (d, 2C), 130.23 (d, 2C), 127.59 (d, 4C), 125.36 (d, 2C), 125.29 (s, 2C), 120.31 (d, 2C), 58.34 (t, 2C), 23.27 (t, 4C), 15.04 ppm (q, 4C); IR (ATR): $\tilde{\nu} = 3063, 3023, 2968, 2933, 2875, 2818, 1649, 1603, 1584, 1478, 1396, 1366, 1351, 1331, 1306, 1275, 1249, 1188, 1160, 1113, 1102, 1052, 1034, 993, 945, 930, 899, 869, 846, 845, 825, 796, 780, 765, 747, 727, 701, 636, 619 \text{ cm}^{-1}$; UV/Vis (CH_2Cl_2): λ_{max} ($\log \epsilon$) = 266 nm (3.89); HR-MS (ESI+) m/z calcd for $\text{C}_{35}\text{H}_{39}\text{N}_2\text{O}$ [M-Br] $^+$: 503.3057, found: 503.3058.

General procedure for the synthesis of amidinium tetrafluoroborates 2a–h

Anion exchange was undertaken by mixing solutions of amidinium bromide (1.0 mmol, in 100 mL acetone) and NaBF_4 (660 mg, 6.0 equiv in 75 mL distilled water) and stirring for 45 minutes at room temperature. Acetone was then evaporated under reduced pressure and the solid was filtered, washed with distilled water (50 mL) taken up in CH_2Cl_2 (50 mL) and dried over Na_2SO_4 . Evaporation of solvent until a minimal amount and adding diethyl ether gave white solids corresponding to tetrafluoroborate salts which were recovered by filtration and dried under vacuum (5.0 mbar) prior to its use on metal-complex syntheses.

2a: Colorless solid; yield: 516 mg (94%); m.p.: > 300 °C; ^1H NMR (400 MHz, CDCl_3): $\delta = 7.81$ (s, 1H), 7.57–7.48 (m, 2H), 7.41–7.34 (m, 4H), 7.09–6.98 (m, 6H), 5.08 (d, $J = 14.7$ Hz, 2H), 4.70 (d, $J = 14.7$ Hz, 2H), 2.30 (s, 6H), 2.27 (s, 6H), 2.19 ppm (s, 6H); ^{13}C NMR (101 MHz, CDCl_3): $\delta = 165.03$ (d, 1C), 141.36 (s, 2C), 139.73 (s, 2C), 138.05 (s, 2C), 135.90 (s, 2C), 133.04 (s, 2C), 132.64 (s, 2C), 131.68 (d, 2C), 131.48 (d, 2C), 130.91 (d, 2C), 130.56 (d, 2C), 129.61 (d, 2C), 129.31 (d, 2C), 59.65 (t, 2C), 21.20 (q, 2C), 19.01 (q, 2C), 17.96 ppm (q, 2C); IR (ATR): $\tilde{\nu} = 3022, 1738, 1649, 1587, 1473, 1442, 1404, 1382, 1348, 1309, 1293, 1260, 1165, 1095, 1050, 1031, 959, 914, 883, 852, 789, 754, 732, 657, 621 \text{ cm}^{-1}$; UV/Vis (CH_2Cl_2): λ_{max} ($\log \epsilon$) = 272 (3.86) nm; HR-MS (ESI+) m/z calcd for $\text{C}_{33}\text{H}_{35}\text{N}_2$ [M- BF_4] $^+$: 459.2795, found: 459.2796.

2b: Colorless solid, yield: 576 mg (94%); m.p.: 279–280 °C; ^1H NMR (500 MHz, CDCl_3): $\delta = 7.91$ (s, 1H), 7.59–7.53 (m, 4H), 7.42 (d, $J = 7.6$ Hz, 2H), 7.39–7.32 (m, 6H), 6.93 (d, $J = 7.6$ Hz, 2H), 5.23 (d, $J = 14.6$ Hz, 2H), 4.71 (d, $J = 14.7$ Hz, 2H), 2.76–2.70 (m, 4H), 1.31 (d, $J = 6.6$ Hz, 6H), 1.27 (d, $J = 6.5$ Hz, 6H), 1.18 (d, $J = 6.6$ Hz, 6H), 1.11 ppm (d, $J = 6.9$ Hz, 6H); ^{13}C NMR (126 MHz, CDCl_3): $\delta = 163.60$ (d, 1C), 147.14 (s, 2C), 143.87 (s, 2C), 139.42 (s, 2C), 136.50 (s, 2C), 132.21 (d, 2C), 131.89 (d, 2C), 131.64 (s, 2C), 131.34 (d, 2C), 129.96 (d, 2C), 129.09 (d, 2C), 127.27 (d, 2C), 125.40 (d, 2C), 61.84 (t, 2C), 29.64 (d, 1C), 29.60 (d, 1C), 29.17 (d, 1C), 29.14 (d, 1C), 27.09 (q, 1C), 27.05 (q, 1C), 25.46 (q, 1C), 25.41 (q, 2C), 25.35 (q, 1C), 22.64 (q, 1C), 22.59 (q, 1C); IR (ATR): $\tilde{\nu} = 3065, 2964, 2931, 2872, 1737, 1626, 1586, 1466, 1440, 1391, 1348, 1325, 1303, 1267, 1238, 1204, 1171, 1053, 934, 919, 854, 810, 778, 755, 728, 699, 667, 632 \text{ cm}^{-1}$; UV/Vis (CH_2Cl_2): λ_{max} ($\log \epsilon$) = 253 (3.76), 273 nm (3.85); HR-MS (ESI+) m/z calcd for $\text{C}_{39}\text{H}_{47}\text{N}_2$ [M- BF_4] $^+$: 543.3734, found: 543.3735.

2c: Pale pinkish solid, yield: 477 mg (92%); m.p.: > 300 °C; ^1H NMR (400 MHz, CDCl_3): $\delta = 8.04$ (s, 1H), 7.53 (td, $J = 7.6, 1.2$ Hz, 2H), 7.40–7.37 (m, 4H), 7.33 (t, $J = 7.6$ Hz, 2H), 7.27–7.22 (m, 4H), 7.06 (d, $J = 8.4$ Hz, 2H), 5.12 (d, $J = 14.7$ Hz, 2H), 4.74 (d, $J = 14.7$ Hz, 2H), 2.34 (s, 6H), 2.27 ppm (s, 6H); ^{13}C NMR (101 MHz, CDCl_3): $\delta = 165.77$ (d, 1C), 140.56 (s, 2C), 139.79 (s, 2C), 136.32 (s, 2C), 133.20 (s, 2C), 133.14 (s, 2C), 131.50 (d, 2C), 131.11 (d, 2C), 131.08 (d, 2C), 130.92 (d, 2C), 129.95 (d, 2C), 129.69 (d, 2C), 129.34 (d, 2C), 59.66 (t, 2C), 19.17 (q, 2C), 18.13 ppm (q, 2C); IR (ATR): $\tilde{\nu} = 3021, 2918, 1647, 1473, 1442, 1402, 1382, 1347, 1309, 1293, 1206, 1165, 1096, 1050, 1030, 998, 959, 914, 883, 852, 789, 773, 753, 732, 657, 620 \text{ cm}^{-1}$; UV/Vis (CH_2Cl_2): λ_{max} ($\log \epsilon$) = 271 nm (3.97); HR-MS (ESI+) m/z calcd for $\text{C}_{31}\text{H}_{31}\text{N}_2$ [M- BF_4] $^+$: 431.2482, found: 431.2489.

2d: Colorless solid, yield: 545 mg (95%); m.p.: 279 °C; ^1H NMR (600 MHz, CDCl_3): $\delta = 7.84$ (s, 1H), 7.54 (t, $J = 7.6$ Hz, 2H), 7.47 (t, $J = 7.8$ Hz, 2H), 7.42–7.35 (m, 4H), 7.31 (t, $J = 6.8$ Hz, 4H), 7.00 (d, $J = 7.6$ Hz, 2H), 5.16 (d, $J = 14.7$ Hz, 2H), 4.69 (d, $J = 14.7$ Hz, 2H), 2.67–2.56 (m, 4H), 2.56–2.43 (m, 4H), 1.24 (t, $J = 7.5$ Hz, 6H), 1.21 ppm (t, $J = 7.5$ Hz, 6H). ^{13}C NMR (151 MHz, CDCl_3): $\delta = 164.09$ (d, 1C), 141.62 (s, 2C), 139.60 (s, 2C), 139.25 (s, 2C), 138.49 (s, 2C), 132.49 (s, 2C), 131.62 (d, 2C), 131.59 (d, 2C), 131.11 (d, 2C), 129.69

(d, 2C), 129.13 (d, 2C), 128.78 (d, 2C), 127.57 (d, 2C), 60.74 (t, 2C), 24.80 (t, 2C), 23.79 (t, 2C), 15.04 (q, 2C), 14.79 (q, 2C); IR (ATR): $\tilde{\nu}$ = 2973, 2937, 2877, 1731, 1642, 1584, 1448, 1411, 1396, 1371, 1351, 1308, 1295, 1240, 1204, 1171, 1093, 1050, 1008, 957, 943, 913, 881, 854, 815, 783, 758, 728, 665, 624 cm^{-1} ; UV/Vis (CH_2Cl_2): λ_{max} ($\log \epsilon$) = 278 nm (3.78); HR-MS (ESI+) m/z calcd for $\text{C}_{35}\text{H}_{39}\text{N}_2$ [$\text{M}-\text{BF}_4$] $^+$: 487.3111, found: 487.3108.

2e: Colorless solid; yield: 512 mg (91%); m.p.: 227 °C; ^1H NMR (400 MHz, CDCl_3): δ = 7.62 (dd, J = 8.2, 0.7 Hz, 1H), 7.40 (td, J = 8.0, 1.7 Hz, 1H), 7.25 (s, 1H), 7.02 (td, J = 7.5, 0.9 Hz, 1H), 6.89 (dd, J = 7.5, 1.5 Hz, 1H), 6.81 (s, 2H), 5.48 (s, 2H), 2.18 (s, 3H), 2.09 ppm (s, 6H); ^{13}C NMR (101 MHz, CDCl_3): δ = 157.87 (d, 1C), 157.19 (s, 2C), 140.57 (s, 2C), 140.18 (s, 2C), 134.67 (s, 4C), 131.68 (d, 2C), 131.17 (d, 2C), 130.45 (d, 4C), 125.54 (d, 2C), 125.37 (s, 2C), 120.45 (d, 2C), 55.72 (t, 2C), 20.93 (q, 2C), 17.46 ppm (q, 4C); IR (ATR): $\tilde{\nu}$ = 2959, 2926, 2869, 1738, 1654, 1605, 1581, 1483, 1454, 1414, 1364, 1237, 1205, 1182, 1059, 1032, 950, 860, 818, 790, 758, 731, 704, 640, 617 cm^{-1} ; UV/Vis (CH_2Cl_2): λ_{max} ($\log \epsilon$) = 246 (3.83), 272 (3.59), 363 nm (2.63); HR-MS (ESI+) m/z calcd for $\text{C}_{33}\text{H}_{35}\text{N}_2\text{O}$ [$\text{M}-\text{BF}_4$] $^+$: 475.2744, found: 475.2744.

2f: Colorless solid; yield: 512 mg (86%); m.p.: 286–287 °C; ^1H NMR (400 MHz, CD_2Cl_2): δ = 7.70 (d, J = 8.3 Hz, 2H), 7.46 (s, 1H), 7.42 (td, J = 8.2, 1.6 Hz, 2H), 7.34 (t, J = 7.8 Hz, 2H), 7.15 (d, J = 7.8 Hz, 4H), 7.05 (td, J = 7.5, 0.9 Hz, 2H), 6.88 (dd, J = 7.6, 1.4 Hz, 2H), 5.46 (br s, 4H), 3.15–2.97 (m, 4H), 1.08 (d, J = 6.8 Hz, 12H), 0.86 ppm (d, J = 6.4 Hz, 12H); ^{13}C NMR (101 MHz, CD_2Cl_2): δ = 157.61 (s, 2C), 157.35 (d, 1C), 145.21 (s, 4C), 139.58 (s, 2C), 131.66 (d, 4C), 130.94 (d, 2C), 125.84 (d, 2C), 125.79 (d, 4C), 124.42 (s, 2C), 121.61 (d, 2C), 57.49 (t, 2C), 28.24 (d, 4C), 25.46 (q, 4C), 23.98 ppm (q, 4C); IR (ATR): $\tilde{\nu}$ = 2969, 2929, 2872, 1647, 1583, 1485, 1469, 1454, 1407, 1388, 1364, 1329, 1299, 1282, 1237, 1186, 1162, 1096, 1029, 932, 900, 879, 848, 812, 788, 767, 748, 699, 657, 639, 617 cm^{-1} ; UV/Vis (CH_2Cl_2): λ_{max} ($\log \epsilon$) = 248 (3.94), 270 (3.73), 312 nm (2.97); HR-MS (ESI+) m/z calcd for $\text{C}_{39}\text{H}_{47}\text{N}_2\text{O}$ [$\text{M}-\text{BF}_4$] $^+$: 559.3683, found: 559.3683.

2g: Colorless solid, yield: 464 mg (87%); m.p.: 281–282 °C; ^1H NMR (400 MHz, CDCl_3): δ = 7.64 (d, J = 7.7 Hz, 2H), 7.41 (td, J = 8.2, 1.7 Hz, 2H), 7.30 (s, 1H), 7.19–7.11 (m, 2H), 7.05–6.98 (m, 6H), 6.87 (dd, J = 7.5, 1.5 Hz, 2H), 5.51 (s, 4H), 2.14 ppm (s, 12H); ^{13}C NMR (101 MHz, CDCl_3): δ = 157.60 (d, 1C), 157.15 (s, 2C), 142.77 (s, 2C), 135.02 (s, 4C), 131.61 (d, 2C), 131.28 (d, 2C), 130.15 (d, 2C), 129.93 (d, 4C), 125.57 (s, 2C), 125.18 (d, 2C), 120.48 (d, 2C), 55.75 (t, 2C), 17.54 (q, 4C); IR (ATR): $\tilde{\nu}$ = 3006, 1656, 1605, 1583, 1485, 1473, 1454, 1436, 1411, 1386, 1362, 1318, 1298, 1240, 1190, 1161, 1057, 1026, 942, 897, 880, 848, 825, 793, 771, 754, 734, 704, 636, 615 cm^{-1} ; UV/Vis (CH_2Cl_2): λ_{max} ($\log \epsilon$) = 250 (3.78), 268 nm (3.62); HR-MS (ESI+) m/z calcd for $\text{C}_{31}\text{H}_{31}\text{N}_2\text{O}$ [$\text{M}-\text{BF}_4$] $^+$: 447.2431, found: 447.2432.

2h: Colorless solid; yield: 464 mg (87%); m.p.: 284 °C; ^1H NMR (400 MHz, CDCl_3): δ = 7.68 (dd, J = 8.2, 0.6 Hz, 2H), 7.40 (td, J = 8.0, 1.7 Hz, 2H), 7.29 (s, 1H), 7.27 (t, J = 7.7 Hz, 2H), 7.09 (d, J = 7.7 Hz, 4H), 6.99 (td, J = 7.5, 0.9 Hz, 2H), 6.85 (dd, J = 7.5, 1.6 Hz, 2H), 5.52 (s, 4H), 2.65–2.45 (m, 8H), 0.97 ppm (t, J = 7.5 Hz, 12H); ^{13}C NMR (101 MHz, CDCl_3): δ = 157.50 (d, 1C), 157.27 (s, 2C), 141.49 (s, 2C), 140.61 (s, 4C), 131.88 (d, 2C), 131.37 (d, 2C), 130.44 (d, 2C), 127.69 (d, 4C), 125.51 (d, 2C), 124.88 (s, 2C), 120.41 (d, 2C), 56.60 (t, 2C), 22.97 (t, 4C) 14.96 ppm (q, 4C); IR (ATR): $\tilde{\nu}$ = 3071, 2968, 2934, 2878, 1650, 1605, 1584, 1480, 1451, 1329, 1246, 1183, 1156, 1105, 1050, 1021, 943, 931, 893, 869, 840, 813, 777, 744, 702, 634, 613 cm^{-1} ; UV/Vis (CH_2Cl_2): λ_{max} ($\log \epsilon$) = 247 (4.04), 272 nm (3.93); HR-MS (ESI+) m/z calcd for $\text{C}_{35}\text{H}_{39}\text{N}_2\text{O}$ [$\text{M}-\text{BF}_4$] $^+$: 503.3057, found: 503.3059.

General procedure for the synthesis of gold(I) NHC complexes 3–10

A 4.5 mL screw-cap vial provided with a stirring bar, was charged with tetrafluoroborate salt (0.10 mmol), $[\text{AuCl}(\text{SMe}_2)]$ (15 mg, 0.05 mmol), $t\text{BuOK}$ (40 mg or 0.35 mL, 1.0 M in THF; 0.35 mmol) and 4 Å molecular sieves (40 mg) in aerobic conditions at room temperature. Vial was sealed with Teflon/silicone septa and purged-backfilled with N_2 three times. After cooling to -78°C , dry degassed THF (3.0 mL) was added to the mixture through a syringe and suspension was stirred overnight, allowing to warm up slowly to room temperature. The resulting suspension was directly filtered through a pad of silica gel (1.5 × 3.0 cm), followed by washing the plug with absolute CH_2Cl_2 (15 mL). The solvent was evaporated, and the residue was taken up in CH_2Cl_2 (2 mL), followed by addition of n -hexane (ca. 35 mL) which gave a cloudy white suspension. The liquid was removed by decantation and solid residue was recrystallized from $\text{CH}_2\text{Cl}_2/n$ -pentane (1:4) to yield pure NHC–AuCl complexes as colorless microcrystalline solids.

Au(9-Mes)Cl 3: Yield: 23 mg (67%); m.p.: 269 °C; ^1H NMR (600 MHz, CDCl_3): δ = 7.37 (t, J = 8.0 Hz, 2H), 7.26 (d, J = 7.6 Hz, 2H), 7.22 (t, J = 7.6 Hz, 2H), 6.98 (s, 2H), 6.89 (s, 2H), 6.85 (d, J = 7.7 Hz, 2H), 4.99 (d, J = 14.9 Hz, 2H), 4.49 (d, J = 14.9 Hz, 2H), 2.27 (d, J = 2.3 Hz, 12H), 2.05 ppm (s, 6H); ^{13}C NMR (151 MHz, CDCl_3): δ = 211.93 (NCN), 142.76 (s, 2C), 139.76 (s, 2C), 138.72 (s, 2C), 136.94 (s, 2C), 134.85 (s, 2C), 133.52 (s, 2C), 131.44 (d, 2C), 130.89 (d, 2C), 129.89 (d, 2C), 129.86 (d, 2C), 129.64 (d, 2C), 128.72 (d, 2C), 59.29 (t, 2C), 21.49 (q, 2C), 19.77 (q, 2C), 18.74 ppm (q, 2C); IR (ATR): $\tilde{\nu}$ = 3950, 3020, 2955, 2921, 2858, 1674, 1634, 1609, 1480, 1436, 1373, 1383, 1303, 1286, 1241, 1208, 1193, 1161, 1122, 1034, 1010, 952, 886, 853, 828, 774, 753, 735, 706, 637 cm^{-1} ; UV/Vis (CH_2Cl_2): λ_{max} ($\log \epsilon$) = 277 (3.98), 335 (3.44), 452 (2.88), 484 nm (2.97); HR-MS (ESI+) m/z calcd for $\text{C}_{33}\text{H}_{34}\text{AuClIN}_2\text{Na}$ [$\text{M}+\text{Na}$] $^+$: 713.1968, found: 713.1972.

Au(9-Dipp)Cl 4: Yield: 20 mg (52%); m.p.: > 300 °C; ^1H NMR (600 MHz, CDCl_3): δ = 7.40 (t, J = 7.7 Hz, 4H), 7.32–7.28 (m, 2H), 7.28–7.25 (m, 2H), 7.24–7.20 (m, 2H), 7.20–7.16 (m, 2H), 6.78 (d, J = 7.6 Hz, 2H), 5.18 (d, J = 14.8 Hz, 2H), 4.54 (d, J = 14.9 Hz, 2H), 2.89–2.75 (m, 4H), 1.38 (d, J = 6.7 Hz, 6H), 1.29 (d, J = 6.9 Hz, 6H), 1.23 (d, J = 6.8 Hz, 6H), 1.11 ppm (d, J = 6.7 Hz, 6H); ^{13}C NMR (151 MHz, CDCl_3): δ = 212.56 (NCN), 147.33 (s, 2C), 144.96 (s, 2C), 142.23 (s, 2C), 139.58 (s, 2C), 133.95 (s, 2C), 131.25 (d, 2C), 130.72 (d, 2C), 130.06 (d, 2C), 129.84 (d, 2C), 128.64 (d, 2C), 126.68 (d, 2C), 124.42 (d, 2C), 61.60 (t, 2C), 29.41 (d, 2C), 29.23 (d, 2C), 26.30 (q, 2C), 25.47 (q, 2C), 25.40 (q, 2C), 23.07 ppm (q, 2C); IR (ATR): $\tilde{\nu}$ = 3060, 3027, 2960, 2925, 2867, 1626, 1588, 1474, 1440, 1386, 1348, 1323, 1300, 1281, 1251, 1226, 1180, 1162, 1125, 1102, 1056, 1015, 960, 948, 935, 887, 811, 778, 767, 754, 729, 666, 639, 620 cm^{-1} ; UV/Vis (CH_2Cl_2): λ_{max} ($\log \epsilon$) = 253 (4.21), 278 nm (3.83); HR-MS (ESI+) m/z calcd for $\text{C}_{39}\text{H}_{46}\text{AuClIN}_2\text{Na}$ [$\text{M}+\text{Na}$] $^+$: 797.2913, found: 797.2923.

Au(9-Xyl)Cl 5: Yield: 16 mg (49%); m.p.: 229–230 °C; ^1H NMR (500 MHz, CDCl_3): δ = 7.38 (t, J = 10.9, 4.1 Hz, 2H), 7.27 (d, J = 7.6 Hz, 2H), 7.23 (t, J = 7.5 Hz, 4H), 7.18 (d, J = 7.6 Hz, 2H), 7.11 (d, J = 7.4 Hz, 2H), 6.85 (d, J = 7.8 Hz, 2H), 5.03 (d, J = 14.9 Hz, 2H), 4.53 (d, J = 14.9 Hz, 2H), 2.31 (s, 6H), 2.12 ppm (s, 6H); ^{13}C NMR (126 MHz, CDCl_3): δ = 214.76 (NCN), 144.87 (s, 2C), 139.48 (s, 2C), 137.00 (s, 2C), 134.49 (s, 2C), 133.79 (s, 2C), 130.68 (d, 2C), 130.46 (d, 2C), 129.54 (d, 2C), 129.45 (d, 2C), 128.93 (d, 2C), 128.86 (d, 2C), 128.51 (d, 2C), 59.05 (t, 2C), 19.57 (q, 2C), 18.56 (q, 2C); IR (ATR): $\tilde{\nu}$ = 3058, 3026, 2987, 2950, 2916, 2858, 2235, 1943, 1871, 1590, 1491, 1434, 1376, 1345, 1290, 1241, 1206, 1181, 1164, 1123, 1094, 1009, 960, 941, 912, 825, 779, 769, 752, 731, 654, 630, 609 cm^{-1} ; UV/Vis (CH_2Cl_2): λ_{max} ($\log \epsilon$) = 281 (3.72), 257 (4.13) nm; HR-MS

(ESI+) m/z calcd for $C_{31}H_{30}AuClIN_2Na$ [M+Na]⁺: 685.1655, found: 685.1676.

Au(9-Dietph)Cl 6: Yield: 13 mg (36%); m.p.: >300 °C; ¹H NMR (600 MHz, CDCl₃): δ = 7.38 (td, J = 7.6, 1.0 Hz, 2H), 7.35 (t, J = 7.7 Hz, 2H), 7.27 (t, J = 8.0 Hz, 4H), 7.20 (t, J = 7.6 Hz, 2H), 7.16 (d, J = 7.6 Hz, 2H), 6.79 (d, J = 7.7 Hz, 2H), 5.10 (d, J = 14.9 Hz, 2H), 4.45 (d, J = 14.9 Hz, 2H), 2.70–2.63 (m, 2H), 2.58–2.50 (m, 2H), 2.50–2.44 (m, 2H), 2.43–2.37 (m, 2H), 1.30 (t, J = 7.5 Hz, 6H), 1.22 ppm (t, J = 7.5 Hz, 6H); ¹³C NMR (151 MHz, CDCl₃): δ = 211.72 (NCN), 144.08 (s, 2C), 142.21 (s, 2C), 139.54 (s, 2C), 139.45 (s, 2C), 134.23 (s, 2C), 130.85 (d, 2C), 129.83 (d, 2C), 129.59 (d, 2C), 129.31 (d, 2C), 128.35 (d, 2C), 128.07 (d, 2C), 126.37 (d, 2C), 60.57 (t, 2C), 25.24 (t, 2C), 23.93 (t, 2C), 14.63 (q, 2C), 14.52 ppm (q, 2C); IR (ATR): $\tilde{\nu}$ = 3063, 3026, 2969, 2924, 2868, 1589, 1476, 1448, 1427, 1388, 1345, 1282, 1226, 1180, 1124, 1108, 1055, 1007, 946, 867, 805, 769, 752, 730, 700, 658, 631 cm⁻¹; UV/Vis (CH₂Cl₂): λ_{max} (log ϵ) = 253 (4.28), 281 nm (3.91); HR-MS (ESI+) m/z calcd for $C_{35}H_{38}AuClIN_2Na$ [M+Na]⁺: 741.2287, found: 741.2297.

Au(10-Mes)Cl 7: Yield: 22 mg (61%); m.p.: 286 °C; ¹H NMR (600 MHz, CD₂Cl₂): δ = 7.25 (t, J = 7.7 Hz, 2H), 7.17 (d, J = 8.1 Hz, 2H), 6.92 (t, J = 8.0 Hz, 2H), 6.89 (s, 4H), 6.58 (d, J = 7.6 Hz, 2H), 4.98 (s, 4H), 2.24 (s, 6H), 2.09 ppm (s, 12H); ¹³C NMR (151 MHz, CD₂Cl₂): δ = 209.32 (NCN), 156.29 (s, 2C), 142.40 (s, 2C), 138.73 (s, 4C), 135.58 (s, 2C), 132.21 (d, 2C), 130.78 (d, 2C), 130.15 (d, 2C), 127.52 (d, 2C), 125.32 (d, 2C), 121.75 (d, 2C), 54.95 (t, 2C), 21.13 (q, 2C), 18.80 ppm (q, 4C); IR (ATR): $\tilde{\nu}$ = 2962, 2920, 2857, 2124, 1722, 1678, 1633, 1605, 1580, 1554, 1484, 1451, 1376, 1261, 1235, 1182, 1105, 1028, 947, 854, 800, 754, 702, 636 cm⁻¹; UV/Vis (CH₂Cl₂): λ_{max} (log ϵ) = 267 (4.03), 278 nm (3.93); HR-MS (ESI+) m/z calcd for $C_{33}H_{34}AuClIN_2NaO$ [M+Na]⁺: 729.1918, found: 729.1922.

Au(10-Dipp)Cl 8: Yield: 28 mg (70%); m.p.: >300 °C; ¹H NMR (600 MHz, CD₂Cl₂): δ = 7.37 (t, J = 7.7 Hz, 2H), 7.27–7.23 (m, 2H), 7.16 (d, J = 7.5 Hz, 4H), 6.92 (t, J = 7.5 Hz, 2H), 6.58 (d, J = 7.6 Hz, 2H), 5.78 (br s, 2H), 4.36 (br s, 2H), 2.91–2.87 (m, 4H), 1.29 (br s, 12H), 0.89 ppm (br s, 12H); ¹³C NMR (151 MHz, CD₂Cl₂): δ = 210.27 (NCN), 156.12 (s, 2C), 146.91 (s, 1C), 145.47 (s, 1C), 142.06 (s, 2C), 132.68 (d, 2C), 131.11 (d, 4C), 129.82 (d, 2C), 127.49 (s, 2C), 126.13 (s, 1C), 125.31 (d, 4C), 124.44 (s, 1C), 121.89 (d, 2C), 56.90 (t, 2C), 29.27 (d, 4C), 25.41 ppm (q, 8C); IR (ATR): $\tilde{\nu}$ = 3063, 2962, 2927, 2868, 1605, 1587, 1454, 1426, 1385, 1352, 1324, 1296, 1272, 1232, 1176, 1111, 1099, 1056, 1018, 957, 942, 932, 888, 877, 819, 800, 762, 738, 638, 611 cm⁻¹; UV/Vis (CH₂Cl₂): λ_{max} (log ϵ) = 271 (4.06) nm; HR-MS (ESI+) m/z calcd for $C_{39}H_{46}AuClIN_2NaO$ [M+Na]⁺: 813.2862, found: 813.2882.

Au(10-Xyl)Cl 9: Yield: 16 mg (48%); m.p.: >300 °C; ¹H NMR (600 MHz, CD₂Cl₂): δ = 7.27 (t, J = 6.9 Hz, 2H), 7.21 (d, J = 8.1 Hz, 2H), 7.18 (t, J = 7.6 Hz, 2H), 7.08 (d, J = 7.5 Hz, 4H), 6.93 (t, J = 6.9 Hz, 2H), 6.58 (d, J = 7.6 Hz, 2H), 5.02 (br s, 4H), 2.14 ppm (s, 12H); ¹³C NMR (151 MHz, CD₂Cl₂): δ = 208.93 (NCN), 156.50 (s, 2C), 145.17 (s, 2C), 136.11 (s, 2C), 132.22 (d, 2C), 130.99 (d, 4C), 129.63 (d, 2C), 128.95 (d, 2C), 127.49 (s, 4C), 125.47 (d, 2C), 121.98 (d, 1C), 121.93 (d, 1C), 55.08 (t, 2C), 18.97 ppm (q, 4C); IR (ATR): $\tilde{\nu}$ = 3068, 2950, 2917, 2859, 1680, 1603, 1574, 1492, 1377, 1343, 1310, 1279, 1236, 1206, 1173, 1159, 1108, 1094, 1034, 1012, 950, 927, 889, 819, 786, 765, 742, 703, 668, 650, 631, 607 cm⁻¹; UV/Vis (CH₂Cl₂): λ_{max} (log ϵ): 261 (3.93), 362 nm (2.31); HR-MS (ESI+) m/z calcd for $C_{31}H_{30}AuClIN_2NaO$ [M+Na]⁺: 701.1605, found: 701.1629.

Au(10-Dietph)Cl 10: Yield: 19 mg (52%); m.p.: 283–285 °C, ¹H NMR (600 MHz, CD₂Cl₂): δ = 7.31 (td, J = 7.6, 3.4 Hz, 2H), 7.28–7.23 (m, 2H), 7.22–7.10 (m, 6H), 6.90 (t, J = 7.5 Hz, 2H), 6.53 (t, J = 7.3 Hz, 1H), 5.01 (br s, 4H), 2.80–2.52 (m, 4H), 2.47–2.24 (m, 4H), 1.18 ppm (t, J = 7.2 Hz, 12H); ¹³C NMR (151 MHz, CD₂Cl₂): δ = 209.83 (NCN), 156.28 (s, 2C), 143.72 (s, 2C), 141.46 (s, 2C), 132.36 (d, 2C), 130.99

(d, 2C), 129.23 (d, 2C), 127.28 (d, 4C), 127.21 (s, 4C), 125.30 (d, 2C), 121.83 (d, 2C), 56.53 (t, 2C), 24.51 (t, 4C), 14.51 ppm (q, 4C). IR (ATR): $\tilde{\nu}$ = 3058, 3031, 2964, 2927, 2868, 1949, 1602, 1577, 1485, 1449, 1427, 1377, 1350, 1296, 1280, 1231, 1206, 1169, 1156, 1101, 1055, 1014, 991, 957, 945, 930, 890, 869, 821, 797, 770, 751, 739, 654, 634 cm⁻¹; UV/Vis (CH₂Cl₂): λ_{max} (log ϵ) = 273 nm (3.87); HR-MS (ESI+) m/z calcd for $C_{35}H_{38}AuClIN_2NaO$ [M+Na]⁺: 757.2236, found: 757.2249.

Experiments for the first catalytic activity evaluation

Procedure A: In an NMR tube, 4-methoxy-*N*-(prop-2-yn-1-yl)benzamide (19 mg, 100 μmol) and hexamethylbenzene (4.1 mg, 25 μmol; internal standard) were dissolved in CDCl₃ (500 μL) and an NMR spectrum was measured. The gold pre-catalyst and AgNTf₂ were added and the tube was shaken vigorously. The yield was determined by integrating the NMR signals against the internal standard.

Procedure B: A 4 mL screw-cap vial was charged with 4-methoxy-*N*-(prop-2-yn-1-yl)benzamide (38 mg, 200 μmol), dodecane (14.1 mg, 100 μmol internal standard) and CHCl₃ (2 mL) under air conditions at room temperature. Then, the gold pre-catalyst and AgNTf₂ (1.0 equiv with respect to gold) were added and reaction mixture was stirred for 24 h at 50 °C in heating bath. The yield was determined by GC-MS peak-analysis of crude mixture against the internal standard.

Acknowledgements

A.C.R. is grateful for a Ph.D. fellowship from Consejo Nacional de Ciencia y Tecnología (México).

Conflict of interest

The authors declare no conflict of interest.

Keywords: carbenes · catalysis · gold · ligands · N-heterocyclic carbenes

- a) A. J. Arduengo, R. L. Harlow, M. Kline, *J. Am. Chem. Soc.* **1991**, *113*, 361–363; b) R. Jazzar, H. Liang, B. Donnadiu, G. Bertrand, *J. Organomet. Chem.* **2006**, *691*, 3201–3205; c) M. Iglesias, D. J. Beetstra, J. C. Knight, L. L. Ooi, A. Stasch, S. Coles, L. Male, M. B. Hursthouse, K. J. Cavell, A. Dervisi, I. A. Fallis, *Organometallics* **2008**, *27*, 3279–3289; d) S. Díez-González, N. Marion, S. P. Nolan, *Chem. Rev.* **2009**, *109*, 3612–3676.
- A. Binobaid, M. Iglesias, D. J. Beetstra, B. Kariuki, A. Dervisi, I. A. Fallis, K. J. Cavell, *Dalton Trans.* **2009**, 7099–7112.
- a) T. Wurm, F. Mulks, C. R. N. Böhlring, D. Riedel, P. Zargaran, M. Rudolph, F. Rominger, A. S. K. Hashmi, *Organometallics* **2016**, *35*, 1070–1078; b) D. Riedel, T. Wurm, K. Graf, M. Rudolph, F. Rominger, A. S. K. Hashmi, *Adv. Synth. Catal.* **2015**, *357*, 1515–1523; c) A. S. K. Hashmi, D. Riedel, M. Rudolph, F. Rominger, T. Oeser, *Chem. Eur. J.* **2012**, *18*, 3827–3830; d) M. J. Spallek, D. Riedel, A. S. K. Hashmi, O. Trapp, *Organometallics* **2012**, *31*, 1127–1132; e) A. S. K. Hashmi, C. Lothschütz, K. Graf, T. Häffner, A. Schuster, F. Rominger, *Adv. Synth. Catal.* **2011**, *353*, 1407–1412; f) A. S. K. Hashmi, C. Lothschütz, C. Böhlring, F. Rominger, *Organometallics* **2011**, *30*, 2411–2417; g) A. S. K. Hashmi, C. Lothschütz, C. Böhlring, T. Hengst, C. Hubbert, F. Rominger, *Adv. Synth. Catal.* **2010**, *352*, 3001–3012; h) A. S. K. Hashmi, T. Hengst, C. Lothschütz, F. Rominger, *Adv. Synth. Catal.* **2010**, *352*, 1315–1337.
- For other highly active gold catalysts, see: M. C. Blanco Jaimes, F. Rominger, M. M. Pereira, R. M. B. Carrilho, S. A. C. Carabineiro, A. S. K. Hashmi, *Chem. Commun.* **2014**, *50*, 4937–4940.

- [5] a) N. Marion, S. P. Nolan, *Chem. Soc. Rev.* **2008**, *37*, 1776–1782; b) J. C. Y. Lin, R. T. W. Huang, C. S. Lee, A. Bhattacharyya, W. S. Hwang, I. J. B. Lin, *Chem. Rev.* **2009**, *109*, 3561–3598; c) M. C. Blanco Jaimes, C. R. N. Böhlring, J. M. Serrano-Becerra, A. S. K. Hashmi, *Angew. Chem. Int. Ed.* **2013**, *52*, 7963–7966; *Angew. Chem.* **2013**, *125*, 8121–8124; d) A. S. K. Hashmi, *Science* **2012**, *338*, 1434; e) A. S. K. Hashmi, *Angew. Chem. Int. Ed.* **2010**, *49*, 5232–5241; *Angew. Chem.* **2010**, *122*, 5360–5369.
- [6] For very interesting book chapters about NHC-gold(I) complexes, see: a) N. Marion, NHC-Copper, Silver and Gold Complexes in Catalysis, in *N-Heterocyclic Carbenes: From Laboratory Curiosities to Efficient Synthetic Tools*, (Ed.: S. Diez-Gonzalez), RSC Publishing, Cambridge, **2010**, ch. 11, pp. 317–336; b) T. Wurm, A. M. Asiri, A. S. K. Hashmi, NHC-Au^I Complexes: Synthesis Activation, and Application, in *N-Heterocyclic Carbenes: Effective Tools for Organometallic Synthesis* (Ed.: S. P. Nolan), Wiley-VCH, Weinheim, **2014**, ch. 9, pp. 243–267.
- [7] a) M. Rudolph, A. S. K. Hashmi, *Chem. Soc. Rev.* **2012**, *41*, 2448–2462; b) C. Hubbert, A. S. K. Hashmi, *Angew. Chem. Int. Ed.* **2010**, *49*, 1010–1012; *Angew. Chem.* **2010**, *122*, 1026–1028; c) S. P. Nolan, *Acc. Chem. Res.* **2011**, *44*, 91–100; d) M. Rudolph, A. S. K. Hashmi, *Chem. Commun.* **2011**, *47*, 6536–6544; e) G. J. Hutchings, A. S. K. Hashmi, *Angew. Chem. Int. Ed.* **2006**, *45*, 7896–7936; *Angew. Chem.* **2006**, *118*, 8064–8105; f) A. S. K. Hashmi, C. Hubbert, *Angew. Chem. Int. Ed.* **2010**, *49*, 1010–1012; *Angew. Chem.* **2010**, *122*, 1026–1028; g) A. Gómez-Suárez, Y. Oonishi, S. Meiries, S. P. Nolan, *Organometallics* **2013**, *32*, 1106–1111; h) for NHC complexes of gold(III), see: M. Pažický, A. Loos, M. João Ferreira, F. Rominger, C. Jäkel, A. S. K. Hashmi, M. Limbach, *Organometallics* **2010**, *29*, 4448–4458; for early results, see: i) A. S. K. Hashmi, L. Schwarz, J.-H. Choi, T. M. Frost, *Angew. Chem. Int. Ed.* **2000**, *39*, 2285–2288; *Angew. Chem.* **2000**, *112*, 2382–2385; j) A. S. K. Hashmi, T. M. Frost, J. W. Bats, *J. Am. Chem. Soc.* **2000**, *122*, 11553–11554; k) A. S. K. Hashmi, R. Salathé, W. Frey, *Chem. Eur. J.* **2006**, *12*, 6991–6996.
- [8] Y. C. Lee, S. Patil, C. Golz, C. Strohmann, S. Ziegler, K. Kumar, H. Waldmann, *Nat. Commun.* **2017**, *8*, 14043.
- [9] a) O. S. Morozov, A. V. Lunchev, A. A. Bush, A. A. Tukov, A. F. Asachenko, V. N. Khrustalev, S. S. Zalesskiy, V. P. Ananikov, M. S. Nechaev, *Chem. Eur. J.* **2014**, *20*, 6162–6170; b) N. Phillips, T. Dodson, R. Tirfoin, J. I. Bates, S. Aldrige, *Chem. Eur. J.* **2014**, *20*, 16721–16731.
- [10] W. Y. Lu, K. J. Cavell, J. S. Wixey, B. Kariuki, *Organometallics* **2011**, *30*, 5649–5655.
- [11] a) J. J. Dunsford, B. M. Kariuki, K. J. Cavell, *Organometallics* **2012**, *31*, 4118–4121; b) M. J. Page, W. Y. Lu, R. C. Poulten, E. Carter, A. G. Algarra, B. M. Kariuki, S. A. Macgregor, M. F. Mahon, K. J. Cavell, D. M. Murphy, M. K. Whittlesey, *Chem. Eur. J.* **2013**, *19*, 2158–2167.
- [12] a) J. J. Dunsford, D. J. Evans, T. Pugh, S. N. Shah, N. F. Chilton, M. J. Ingleson, *Organometallics* **2016**, *35*, 1098–1106; b) J. W. Hall, D. M. L. Unson, P. Brunel, L. R. Collins, M. K. Cybulski, M. F. Mahon, M. K. Whittlesey, *Organometallics* **2018**, *37*, 3102–3110; c) F. Sebest, J. J. Dunsford, M. Adams, J. Pivot, P. D. Newman, S. Diez-Gonzalez, *ChemCatChem* **2018**, *10*, 2041–2045; d) G. A. Chesnokov, M. A. Topchiy, P. B. Dzhevakov, P. S. Gribanov, A. A. Tukov, V. N. Khrustalev, A. F. Asachenkov, N. S. Nechaev, *Dalton Trans.* **2017**, *46*, 4331–4345; e) Q. Teng, W. Wu, H. A. Duong, H. V. Huynh, *Chem. Commun.* **2018**, *54*, 6044–6047; f) A. R. Leverett, A. I. McKay, M. L. Cole, *Dalton Trans.* **2015**, *44*, 498–500; g) R. Collins, T. M. Rookes, M. F. Mahon, I. M. Riddlestone, M. K. Whittlesey, *Organometallics* **2014**, *33*, 5882–5887; h) J. J. Dunsford, D. S. Tromp, C. J. Elsevier, K. J. Cavell, B. M. Kariuki, *Dalton Trans.* **2013**, *42*, 7318–7329; i) P. Hauwert, J. J. Dunsford, D. S. Tromp, J. J. Weigand, M. Lutz, K. J. Cavell, C. J. Elsevier, *Organometallics* **2013**, *32*, 131–140; j) M. Iglesias, D. J. Beetstra, A. Stasch, P. N. Horton, M. B. Hursthouse, S. J. Coles, K. J. Cavell, A. Dervisi, I. A. Fallis, *Organometallics* **2007**, *26*, 4800–4809.
- [13] a) K. R. Sampford, J. L. Carden, E. B. Kidner, A. Berry, K. J. Cavell, D. M. Murphy, B. M. Kariuki, P. D. Newman, *Dalton Trans.* **2019**, *48*, 1850–1858; b) A. Kumar, D. Yuan, H. V. Huynh, *Inorg. Chem.* **2019**, *58*, 7545–7553; c) T. T. Lam, H. T. T. Luong, H. V. Huynh, *RSC Adv.* **2018**, *8*, 34960–34966.
- [14] S. Flügge, A. Anoop, R. Goddard, W. Thiel, A. Fürstner, *Chem. Eur. J.* **2009**, *15*, 8558–8565.
- [15] a) S. Saba, A. M. Brescia, M. K. Kaloustian, *Tetrahedron Lett.* **1991**, *32*, 5031–5034; b) L. R. Orelli, M. B. Garcia, I. A. Perillo, *Heterocycles* **2000**, *53*, 2437–2450.
- [16] E. L. Kolychev, I. A. Portnyagin, V. V. Shuntikov, V. N. Khrustalev, M. S. Nechaev, *J. Organomet. Chem.* **2009**, *694*, 2454–2462.
- [17] CCDC 1918016 (**1b**), 1918017 (**1c**), 1918018 (**1f**), 1918019 (**1g**), 1918020 (**3**), 1918021 (**4**), 1918022 (**6**) and 1918023 (**7**) contain the supplementary crystallographic data for this paper. These data are provided free of charge by The Cambridge Crystallographic Data Centre.
- [18] Experiments under conditions presented in Table 4, in the absence of AuCl(SMe₂) were firstly carried out.
- [19] M. R. Fructos, T. R. Belderrain, P. de Frémont, N. M. Scott, S. P. Nolan, M. M. Diaz-Requejo, P. J. Perez, *Angew. Chem. Int. Ed.* **2005**, *44*, 5284–5288; *Angew. Chem.* **2005**, *117*, 5418–5422.
- [20] A. Poater, F. Ragone, R. Mariz, C. Dorta, L. Cavallo, *Chem. Eur. J.* **2010**, *16*, 14348–14353.
- [21] P. De Frémont, N. M. Scott, E. D. Stevens, S. P. Nolan, *Organometallics* **2005**, *24*, 2411–2418.
- [22] A. R. Choudhury, K. Islam, M. T. Kirchner, G. Mehta, T. N. Guru-Row, *J. Am. Chem. Soc.* **2004**, *126*, 12274–12275.
- [23] a) A. Poater, F. Ragone, S. Giudice, C. Costabile, R. Dorta, S. P. Nolan, L. Cavallo, *Organometallics* **2008**, *27*, 2679–2681; b) H. Clavier, S. P. Nolan, *Chem. Commun.* **2010**, *46*, 841–861.
- [24] A. Poater, L. Falivene, C. A. Urbina-Blanco, S. Manzini, S. P. Nolan, L. Cavallo, *Dalton Trans.* **2013**, *42*, 7433–7439.
- [25] a) A. Poater, B. Cosenza, A. Correa, S. Giudice, F. Ragone, V. Scarano, L. Cavallo, *Eur. J. Inorg. Chem.* **2009**, 1759–1766; b) L. Falivene, R. Credendino, A. Poater, A. Petta, L. Serra, R. Oliva, V. Scarano, L. Cavallo, *Organometallics* **2016**, *35*, 2286–2293; c) Parameters for SambVca 2.0 calculations: $r=3.5 \text{ \AA}$, $d=2.0 \text{ \AA}$, mesh spacing = 0.10, bond radii scaled by 1.17 and hydrogen atoms were omitted. For direct comparison, listed parameters are identical to those of the examples found in literature.
- [26] A. Collado, J. Balogh, S. Meiries, A. M. Z. Slawin, L. Falivene, L. Cavallo, S. P. Nolan, *Organometallics* **2013**, *32*, 3249–3252.
- [27] A. Gómez-Suárez, R. S. Ramón, O. Songis, A. M. Z. Slawin, C. S. J. Cazin, S. P. Nolan, *Organometallics* **2011**, *30*, 5463–5470.
- [28] S. R. Patrick, A. Collado, S. Meiries, A. M. Z. Slawin, S. P. Nolan, *J. Organomet. Chem.* **2015**, *775*, 152–154.
- [29] O. S. Morozov, P. S. Gribanov, A. F. Asachenko, P. V. Dorovatovskii, V. N. Khrustalev, V. B. Rybakov, M. S. Nechaev, *Adv. Synth. Catal.* **2016**, *358*, 1463–1468.
- [30] a) J. P. Weyrauch, W. Frey, J. W. Bats, A. S. K. Hashmi, *Org. Lett.* **2004**, *6*, 4391–4394; b) A. M. Schuster, M. Schmuck, F. Rominger, A. S. K. Hashmi, *Eur. J. Org. Chem.* **2011**, *24*, 4595–4602.
- [31] a) J. P. Weyrauch, A. S. K. Hashmi, A. Schuster, T. Hengst, S. Schetter, A. Littmann, M. Rudolph, M. Hamzic, J. Visus, F. Rominger, W. Frey, J. W. Bats, *Chem. Eur. J.* **2010**, *16*, 956–963; compare also: b) A. S. K. Hashmi, M. C. Blanco Jaimes, A. M. Schuster, F. Rominger, *J. Org. Chem.* **2012**, *77*, 6394–6408; c) A. S. K. Hashmi, A. Littmann, *Chem. Asian J.* **2012**, *7*, 1435–1442; d) A. S. K. Hashmi, M. Rudolph, S. Schymura, J. Visus, W. Frey, *Eur. J. Org. Chem.* **2006**, 4905–4909.
- [32] S. Tšupova, M. Rudolph, F. Rominger, A. S. K. Hashmi, *Adv. Synth. Catal.* **2016**, *358*, 3999–4005.
- [33] F. Izquierdo, S. Manzini, S. P. Nolan, *Chem. Commun.* **2014**, *50*, 14926–14937.
- [34] G. M. Sheldrick, *Acta Crystallogr. Sect. A* **2015**, *71*, 3–8.
- [35] G. M. Sheldrick, *Acta Crystallogr. Sect. C* **2015**, *71*, 3–8.

Manuscript received: May 29, 2019

Accepted manuscript online: July 16, 2019

Version of record online: August 8, 2019